



**Pacific Northwest**  
NATIONAL LABORATORY

*Proudly Operated by Battelle Since 1965*

# Standard High Solids Vessel Design Non-Newtonian Simulant Qualification

**March 2017**

CA Burns  
RC Daniel  
PA Gauglitz

PP Schonewill  
SD Hoyle  
RA Peterson

## DISCLAIMER

This report was prepared as an account of work sponsored by an agency of the United States Government. Neither the U. S. Government nor any agency thereof, nor Battelle Memorial Institute, nor any of their employees, makes any warranty, express or implied, or assumes any legal liability or responsibility for the accuracy, completeness, or usefulness of any information, apparatus, product, or process disclosed for any uses other than those related to WTP for DOE, or represents that its use would not infringe privately owned rights. Reference herein to any specific commercial product, process, or service by trade name, trademark, manufacturer, or otherwise does not necessarily constitute or imply its endorsement, recommendation, or favoring by the United States Government or any agency thereof, or Battelle Memorial Institute, and nothing herein is intended to create any right or benefit enforceable by a third party. The views and opinions of authors expressed herein do not necessarily state or reflect those of the United States Government or any agency thereof.

PACIFIC NORTHWEST NATIONAL LABORATORY  
*operated by*  
BATTELLE  
*for the*  
UNITED STATES DEPARTMENT OF ENERGY  
*under Contract DE-AC05-76RL01830*

Printed in the United States of America

Available to DOE and DOE contractors from the  
Office of Scientific and Technical Information,  
P.O. Box 62, Oak Ridge, TN 37831-0062;  
ph: (865) 576-8401  
fax: (865) 576-5728  
email: [reports@adonis.osti.gov](mailto:reports@adonis.osti.gov)

Available to the public from the National Technical Information Service  
5301 Shawnee Rd., Alexandria, VA 22312  
ph: (800) 553-NTIS (6847)  
email: [orders@ntis.gov](mailto:orders@ntis.gov) <<http://www.ntis.gov/about/form.aspx>>  
Online ordering: <http://www.ntis.gov>



This document was printed on recycled paper.

(8/2010)

# **Standard High Solids Vessel Design Non-Newtonian Simulant Qualification**

CA Burns	PP Schonewill
RC Daniel	SD Hoyle
PA Gauglitz	RA Peterson

March 2017

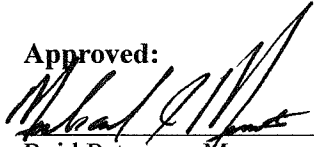
Prepared for  
the U.S. Department of Energy  
under Contract DE-AC05-76RL01830

Pacific Northwest National Laboratory  
Richland, Washington 99352

## COMPLETENESS OF TESTING

*This report describes the results of work and testing specified by Test Plan TP-WTPSP-132, Rev 1.0. The work and any associated testing followed the quality assurance requirements outlined in the Test Plan. The descriptions provided in this test report are an accurate account of both the conduct of the work and the data collected. Test plan results are reported. Also reported are any unusual or anomalous occurrences that are different from expected results. The test results and this report have been reviewed and verified.*

Approved:



Delegate  
for

Reid Peterson, Manager  
WTP R&T Support Project

April 4, 2017

Date

## Executive Summary

The Hanford Tank Waste Treatment and Immobilization Plant (WTP) is working to develop a Standard High Solids Vessel Design process vessel. To support testing of this new design, WTP engineering staff requested that a non-Newtonian simulant be developed that would represent the Most Adverse Design Condition (MADC), denoted as MADC-4, with respect to mixing performance as specified by WTP. The majority of the simulant requirements are specified in 24590-PTF-RPT-PE-16-001, Rev. 0,<sup>1</sup> and a discussion of suggested non-Newtonian rheological parameters for the simulant was provided in WTP-RPT-241, Rev. 0.<sup>2</sup>

This document describes the simulant composition that will satisfy the basis requirement along with ancillary testing to assess the rheological behavior of the simulant depending on the formulation approach used, simulant aging, and the effects of dilution. From this data, a simulant recipe to meet the basis is recommended. The simulant recipe was designed to meet a target rheology (as expressed by Bingham model parameters) of  $34.5 \pm 1.5$  Pa [yield stress] and  $33.5 \pm 1.5$  cP [consistency] at 25 °C.

### MADC-4 Non-Newtonian Simulant

The composition of the MADC-4 non-Newtonian simulant is as follows:

1. Non-Newtonian carrier fluid consisting of (nominally) 35.7 wt% 80/20 Kaolin/Bentonite Clay, 0.09 wt% NaCl, and 100 ppmv Biotrol-509 (Biocide, 5 wt% 2,2-dibromo-3-nitrilpropionamide, DBNPA) dissolved in Richland city water. The non-Newtonian carrier fluid comprises 96.65 wt% of the simulant.
2. 3.35 wt% of the larger ( $> 100 \mu\text{m}$ ) and denser particles from the MADC-1 simulant solids in the carrier fluid consisting of the components identified in Table ES.1. These solids, to avoid conflating them with other simulant materials, are referred to as the larger, denser spike particles (LDSP).

---

<sup>1</sup> Slaathaug E. 2016. *Basis for Simulant Properties for Standard High Solids Vessel Mixing Testing*. 24590-PTF-RPT-PE-16-001, Rev. 0, Bechtel National, Inc., Richland, Washington.

<sup>2</sup> Peterson RA et al. 2016. *Simulant Basis for the Standard High Solids Vessel Design*. RPT-WTP-241. Pacific Northwest National Laboratory, Richland, Washington

**Table ES.1.** LDSP components for the MADC-4 simulant.

Component	Supplier Description	Sieve Cut Mesh, (Micron)	Particle Size, d(50) (microns)	Particle Density (g/mL)	Mass Fraction (%)
Basalt	Dresser Trap Rock, Inc. Manufactured Sand #40 Product 812 (sieved to pass through a 45 mesh sieve and retained on a 50 mesh sieve)	-45/+50 (-350 μm/+300 μm)	442	3.00	0.25
Zirconium oxide (Zirox)	Washington Mills (Durazon) Zirox -100/+170 (sieved and retained on a 140 mesh)	-100/+140 -150 μm/+106 μm	149	5.78	3.10

The bulk density of the carrier fluid without adding the LDSP is 1.274 g/mL; and with the LDSP added the bulk density is 1.307 g/mL. The LDSP were not found to impact the rheological parameters appreciably, and so all Bingham parameters reported were measured with the LDSP present unless noted. The range of Bingham parameters determined for the recommended recipe is given in Table ES.2 as a function of elapsed time from when the samples were prepared. The values are taken from five samples with the same composition.

**Table ES.2.** Mean Bingham parameters of recommended simulant.

Time Since Sample Preparation	Mean Yield Stress <sup>(a)</sup> (Pa)	Standard Deviation in Yield Stress (Pa)	Mean Consistency <sup>(a)</sup> (cP)	Standard Deviation in Consistency (cP)
< 15 days	36.7	3.5	32.4	1.4
15 to 25 days	32.6	1.2	33.0	0.5
25 to 35 days	33.9	2.0	36.3	2.5
> 35 days	35.2	2.0	35.9	1.7

(a) Parameters taken from the second down ramp over the range 250 to 800 s<sup>-1</sup>.

## Acronyms and Abbreviations

BNI	Bechtel National, Inc.
BOD	basis of design
HASQARD	Hanford Analytical Services Quality Assurance Requirements Documents
LDSP	larger, denser spike particles
MADC	Most Adverse Design Condition
NIST	National Institute of Standards and Technology
NN	non-Newtonian
PNNL	Pacific Northwest National Laboratory
PSD	particle size distribution
QA	quality assurance
QC	quality control
RCW	Richland city water
R&D	research and development
SHSVD	Standard High Solids Vessel Design
WTP	Hanford Tank Waste Treatment and Immobilization Plant
WTPSP	Waste Treatment Plant Support Program



## Contents

Executive Summary .....	v
MADC-4 Non-Newtonian Simulant .....	v
Acronyms and Abbreviations .....	vii
1.0 Introduction .....	1.1
1.1 Target Requirements for the MADDC-4 Simulant .....	1.1
1.2 Simulant Development Process .....	1.2
1.3 Testing Requirements .....	1.2
1.4 Quality Requirements .....	1.4
1.5 Report Organization .....	1.5
2.0 Simulant Preparation and Characterization Methods .....	2.1
2.1 Simulant Preparation .....	2.1
2.2 Characterization Methods .....	2.3
2.2.1 Rheology .....	2.3
2.2.2 Density .....	2.6
2.2.3 Particle Size Analysis .....	2.7
2.2.4 Solids Content .....	2.7
3.0 Non-Newtonian Simulant: Testing and Results .....	3.1
3.1 Initial Parametric Study .....	3.1
3.2 Refinement from Parametric Data .....	3.4
3.3 Selection of the Recommended Simulant .....	3.5
3.3.1 Effect of Preparation Sequencing .....	3.6
3.3.2 Effect of Sample Aging .....	3.9
3.4 Rheology of the Recommended Simulant .....	3.12
3.5 Simulant Technical Concerns and Recommendations .....	3.15
3.6 Dry Basis of Recommended Simulant .....	3.17
4.0 Other Properties of the Recommended Simulant .....	4.1
4.1 Impact of Dilution .....	4.1
4.2 Impact of Temperature on Rheology .....	4.7
4.3 Simulant Sieving .....	4.8
5.0 Summary and Conclusions .....	5.1
6.0 References .....	6.1
Appendix A Rheograms of the Recommended Simulant .....	A.1
Appendix B Summary of Non-Newtonian Simulant Rheology .....	B.1

## Figures

Figure 2.1. Particle size distribution of sieved components of the LDSP, pre-sonication and post-sonication.....	2.2
Figure 2.2. Rotor and cup geometry used in rotational viscometry testing used for simulant development.....	2.5
Figure 2.3. Summary of flow curve behaviors typically observed for concentrated slurries, including (a) common time-independent behaviors, (b) static and dynamic yield stress, and (c) flow-curve hysteresis.....	2.6
Figure 3.1. Measured rheological parameters of the initial parametric samples compared to the rheological parameter targets (shown as a black circle surrounded by a dotted line).....	3.3
Figure 3.2. Bingham yield stress versus nominal clay solids concentration for parametric samples NN-005 through NN-008 (0.10 wt%) and NN-013 through NN-016 (0.05 wt%). The target yield stress (black line) is shown for reference.....	3.3
Figure 3.3. Bingham rheology parameters for refined simulant compositions. Note that the “best estimate” sample was prepared in triplicate (open squares). .....	3.5
Figure 3.4. Rheological parameters of “best” recipe samples measured between 8 to 12 days. The data is included from samples NN-022, NN-026, NN-027, NN-028, and NN-029. The white square with error bars represents the mean of the five samples and the associated standard deviations of the mean.....	3.9
Figure 3.5. Aggregated yield stress for the “best” recipe over time. Since the aggregation is based on discrete data, the aggregated data (solid line) represents a mean value in 2-day increments, with lower and upper bounds (dotted lines) representing a standard deviation of the mean.....	3.10
Figure 3.6. Aggregated consistency for the “best” recipe over time. Since the aggregation is based on discrete data, the aggregated data (solid line) represents a mean value in 2-day increments, with lower and upper bounds (dotted lines) representing a standard deviation of the mean.....	3.11
Figure 3.7. Flow curves for NN-028 after 21 days of aging showing all three consecutive flow curves on the same plot (A) and individually (B – first, C – second, and D – third). Individual flow curves show the best-fit Bingham plastic for a shear rate range of 250 to 800 $s^{-1}$ (solid black line) and extrapolated to the full range of shear rates measured (dashed line).....	3.14
Figure 4.1. Parity plots demonstrating the accuracy of non-Newtonian simulant (A) density and (B) total solids concentration measurements. Calculated values are based on the known simulant composition and component densities.....	4.2
Figure 4.2. Calculated sample dilution ratio $X$ as a function of (A) diluted sample density $\rho f$ and (B) diluted sample total solids concentration $xTS(f)$ . Calculation results are shown for both the exact analysis (open circles) and approximate correlations (Eqs. (4.14) and (4.15) – solid lines). .....	4.5
Figure 4.3. Measured NN-027c non-Newtonian slurry rheology as a function of dilution ratio: (A) Bingham yield stress and (B) Bingham consistency. Bingham plastic constitutive equation parameters were derived by fitting down-ramp flow curve data over shear rates of 250 to 800 $s^{-1}$ .....	4.7
Figure 4.4. Non-Newtonian simulant rheology as a function of temperature: (A) Bingham yield stress and (B) Bingham consistency. Bingham plastic constitutive equation parameters were	

derived by fitting down-ramp flow curve data over shear rates of 250 to 800 s<sup>-1</sup>. Results are shown for the simulant with (sample NN-028) and without (sample NN-029) LDSP. .... 4.8

Figure 4.5. Images of sieved fractions of the 80:20 bentonite:kaolin clay mixture used in the MADC-4 non-Newtonian simulant. Left: 106 μm sieve cut, Right: 425 μm sieve cut. .... 4.9

Figure 4.6. Images of sieved fractions of the MADC-4 non-Newtonian simulant. From left to right: 106 μm sieve cut (Zirox solids and clay cross-over product; see Figure 4.5), 300 μm sieve cut (basalt solids), and 425 μm sieve cut (large clay particles; see Figure 4.5)..... 4.10

## Tables

Table 1.1. Modifications to BNI Guideline testing. <sup>(a)</sup> .....	1.3
Table 2.1. MADC-4 simulant component information.....	2.3
Table 2.2. Summary of Malvern Mastersizer 2000 instrument information.....	2.7
Table 3.1. Composition of initial parametric samples.....	3.2
Table 3.2. Composition of refined simulant samples.....	3.4
Table 3.3. Composition of samples NN-024, NN-025, and NN-026.....	3.6
Table 3.4. Sequencing variants of “best” recipe NN-022.....	3.7
Table 3.5. Measured Bingham parameters of sequencing variants.....	3.8
Table 4.1. Properties assumed for the undiluted “best” simulant recipe (based on sample NN-027c) for the dilution calculations shown in Figure 4.2.....	4.5
Table 4.2. Measured physical properties of undiluted, 10% diluted, and 20% diluted non-Newtonian simulant (sample NN-027c).....	4.6
Table 4.3. Summary of results for dilution ratio inference by pycnometer density, graduated cylinder density, and total solids concentration for the diluted non-Newtonian simulant (sample NN-027c).....	4.6
Table 4.4. Sieving results for 1 L of non-Newtonian simulant with (sample NN-031b) and without (sample NN-032b) LDSP demonstrating clay crossover of target basalt and Ziroy sieve cuts.....	4.9
Table 5.1. Summary of recommended recipe (dry-basis) and properties for the MADC-4 non-Newtonian simulant.....	5.2

## 1.0 Introduction

This document provides the composition and properties of the proposed non-Newtonian simulant for the Standard High Solids Vessel Design (SHSVD) testing for the Hanford Tank Waste Treatment and Immobilization Plant (WTP). The non-Newtonian simulant was developed in accordance with the basis described by Peterson et al. (2016) and is intended to represent the Most Adverse Design Condition 4 (MADC-4) in the SHSVD vessels (Slaathaug 2016). It consists of a carrier fluid with selected larger, denser spike particles (LDSP) from the MADC-1 Newtonian simulant (Fiskum et al. 2017) and has rheological parameters within the basis of design (BOD).

The non-Newtonian simulant was not developed with the intent of representing any particular waste stream/feed vector to the WTP. Thus, the non-Newtonian simulant is purely a physical simulant for the purposes of obtaining certain rheological target parameters. The scope of the mixing requirements verification tests to be performed with this simulant will be defined in the *Subsystems Requirements Report*, 24590-WTP-ES-ENG-14-012, Rev. 1,<sup>1</sup> and the Test Specification, 24590-WTP-RPT-ENG-16-001.

### 1.1 Target Requirements for the MADC-4 Simulant

The requirements for the MADC-4 simulant are provided by Slaathaug (2016). The MADC-4 simulant is a non-Newtonian slurry with rheology at the upper SHSVD vessel limits and with the largest/most dense solid particles present [i.e., the simulant should include a quantity of the largest/most dense particles from the MADC-1 simulant (Zirox and basalt)]. These spike particles are referred to as the large, density spike particles, or LDSP, throughout the remainder of this document. The most critical parameter for the MADC-4 simulant is the Bingham rheology. The density of the MADC-4 simulant is not required to meet any particular target value. The proposed physical properties for the MADC-4 simulant described in Section 7.0 of Slaathaug (2016) are:

1. Slurry rheology: 33 Pa (yield stress)/32 cP (consistency). This “[assures meeting the 30 Pa / 30 cP basis of design (BOD) requirement].”
2. Solid concentration: N/A
3. Specific particles: spike simulant with two times the mass of particles (total grams of particles per liter of simulant)  $\geq 100 \mu\text{m}$  as was used in the MADC-1 simulant.
4. Slurry density: 1.0 – 1.3 g/mL. This range is expected and is not considered a requirement for the simulant.

Note that the rheological parameters quoted in Item 1 were to be met after the addition of the spike particles, e.g., LDSP, described in Item 3. A target rheological working range of  $34.5 \pm 1.5$  Pa and  $33.5 \pm$

---

<sup>1</sup> Peurrung L and W Donigan. *2016 Standard High Solids Vessel Design (SHSVD) Test Specification*. 24590-WTP-ES-ENG-14-012, Rev. 1. Bechtel National, Inc., Richland, Washington.

1.5 cP<sup>1</sup> was defined for the PNNL MADC-4 non-Newtonian simulant development activities. This working range has the following aspects:

1. Quantitatively defines what PNNL considers an acceptable simulant rheology
2. Increases confidence that the PNNL developed recipe will be above the MADC-4 targets for non-Newtonian yield stress and consistency (33 Pa and 32 cP, respectively, per Josephson 2016<sup>2</sup>)
3. Provides upper rheology limits to avoid grossly exceeding the MADC-4 targets

## 1.2 Simulant Development Process

Simulant iterations were required for the development of the MADC-4 non-Newtonian carrier fluid. There was no iteration on the LDSP as these were previously defined along with the rest of the MADC-1 solids (Slaathaug 2016; Peterson et al 2016). The development process is summarized as follows.

The MADC-4 non-Newtonian carrier fluid was developed by preparing a variety of slurries while varying the ratios of clay solids, salt, and Richland city water (RCW). The clay was composed of both kaolin and bentonite, with the ratio of kaolin to bentonite always fixed at 4:1. After preparation, physical property data (density, moisture content, and rheology) were measured. Adjustments to the carrier fluid composition were made based on the physical property data collected, which was primarily guided by the rheological parameters. Once a simulant composition was prepared that was within the bounds of the target rheology, that composition was assessed in a few other important areas:

- Rheological behavior with and without LDSP
- Effect of simulant aging on rheology, i.e., evolution of Bingham parameters with time
- Effect of temperature on rheology
- Effect of preparation sequencing on rheology
- Response of simulant to dilution with water

Once these assessments were completed, the simulant development process was considered complete.

## 1.3 Testing Requirements

Where possible, all testing was conducted in compliance with the Bechtel National, Inc. (BNI) document *Guidelines for Performing Chemical, Physical, and Rheological Properties Measurements*, 24590-WTP-GPG-RTD-001 (Smith and Prindiville 2002; hereafter called the BNI Guideline). The BNI Guideline was developed for actual waste testing and as such was somewhat limited. PNNL instituted several exceptions to the BNI Guideline as delineated in Table 1.1. The rationale for the modification is also provided in Table 1.1, which mostly results in a more accurate measurement.

---

<sup>1</sup> Burns CA. 2016. *Non-Newtonian Simulants for the Standard High Solids Vessel Design (SHSVD)*. PP-WTPSP-145, Rev. 0.0, Pacific Northwest National Laboratory, Richland, WA.

<sup>2</sup> Josephson, G. 2016. *Non-Newtonian Rheology Uncertainty*. CALC No. 24590-PTF-MVC-M59T-000001 Rev. 0

Work at PNNL was conducted according to the PNNL Test Plan TP-WTPSP-132, Rev 1.0, *Test Plan for PNNL WTPSP-QA Program Support of High Solids Vessel Testing*,<sup>1</sup> and the PNNL Project Plan PP-WTPSP-145, Rev 0.0, *Non-Newtonian Simulants for the Standard High Solids Vessel Design*.<sup>2</sup>

The scope presented in this report was executed under the Test Instruction, TI-WTPSP-152, *Non-Newtonian Simulant Makeup and Physical Property Measurements*. Due to time constraints, some of the original scope outlined in PP-WTPSP-145, Rev 0.0, was not executed.

**Table 1.1.** Modifications to BNI Guideline testing.<sup>(a)</sup>

Guideline Requirement	Modified Implementation <sup>(b)</sup>	Rationale
Physical properties Section 4.4 (Note) requires that all masses are to be recorded to the nearest milligram.	PNNL will measure components on balances that are appropriate to the total measured mass. In cases where small quantities are measured, mass will be recorded to the nearest milligram or tenth of milligram. In cases where the component is >5 g, mass may be measured to the nearest 10 milligrams (0.01 g). In cases where >1000 g mass is recorded, the mass will be measured to the nearest 100 mg (0.1 g).	The nearest milligram mass measurement makes sense for small mass samples and containers. It is not achievable where the analytical balance capacity would be exceeded and a higher capacity balance (reduced figures past decimal) is required. In all cases, masses recorded that don't meet the nearest milligram requirement will be recorded with at least 3 significant figures.
The BNI Guidelines Section 5.3 requires the use of NIST-traceable <sup>(c)</sup> viscosity standards.	PNNL will purchase certified viscosity reference standards from Cannon Instrument Company or Poulten Selfe and Lee Ltd. The Cannon Instrument Company was delegated by NIST in 2003 for the responsibility for US national standards for certified liquid viscosity reference material.	Direct NIST-traceable viscosity standards are not commercially available. The production of viscosity reference material is performed by measurement with a certified master viscometer, not by comparison to a certified reference material.
Per Section 5.6, fitting shear stress versus shear rate data is to be fitted to three non-Newtonian models (Oswald, Bingham Plastic, Herschel-Bulkley). Further, the shear stress versus shear rate is to	PNNL will fit the non-Newtonian simulant to the Bingham Plastic model. PNNL will test at 25 °C for the parametric test samples. Once a formulation is selected, testing	If other models are required they can be requested, there is too much data presented here to analyze using 3 different models. Testing at 40 °C does not reflect the test conditions at the SHSVD platform. The temperature range of 10 to 30 °C is

<sup>1</sup> Minette, MJ. 2015. *Test Plan for PNNL WTPSP-QA Program Support of High Solids Vessel Testing*. TP-WTPSP-132, Rev 1.0, Pacific Northwest National Laboratory, Richland, WA.

<sup>2</sup> Burns, CA. 2016. *Non-Newtonian Simulants for the Standard High Solids Vessel Design*. PP-WTPSP-145, Rev 0.0, Pacific Northwest National Laboratory, Richland, WA.

Guideline Requirement	Modified Implementation <sup>(b)</sup>	Rationale
be measured at 25 and 40 °C. Testing is to be conducted twice on each sample and at least duplicate samples are to be tested.	will be conducted at 10, 15, 20, 25, and 30 °C.  PNNL will conduct single sample tests just once during parametric studies. The final selected formulation will be tested in duplicate and each duplicate sample in replicate.	consistent with the temperature the SHSVD will be exposed to.  It is not necessary (waste of resources) to obtain multiple data sets on formulations that we won't use.

(a) SM Barnes, WTP, approved these exceptions via email on July 26, 2016.

(b) Modifications made to reflect what was implemented for non-Newtonian simulant development.

(c) NIST = National Institute of Standards and Technology.

## 1.4 Quality Requirements

PNNL complies with the requirements found in the following standards and implements them in their Waste Treatment Plant Support Program (WTPSP) Quality Assurance (QA) Program:

- ASME NQA-1-2000, *Quality Assurance Requirements for Nuclear Facility Applications*, Part I, Requirements for Quality Assurance Programs for Nuclear Facilities
- ASME NQA-1-2000, Part II, Subpart 2.7, Quality Assurance Requirements for Computer Software for Nuclear Facility Applications
- ASME NQA-1-2000, Part IV, Subpart 4.2, Guidance on Graded Application of Quality Assurance (QA) Requirements for Nuclear-Related Research and Development

This project recognizes that QA applies in varying degrees to a broad spectrum of research and development (R&D) in the technology life cycle. The WTPSP uses a graded approach for the application of the QA controls such that the level of analysis, extent of documentation, and degree of rigor of process control are applied commensurate with their significance, importance to safety, life cycle state of work, or programmatic mission. The technology life cycle is characterized by flexible and informal QA activities in basic research, which becomes more structured and formalized through the applied R&D stages.

The processes and work used as input to this report were conducted at the “Applied Research” level. Applied Research consists of research tasks that acquire data and documentation necessary to assure satisfactory reproducibility of results. The emphasis during this stage of a research task is on achieving adequate documentation and controls necessary to be able to reproduce results.

Analytical work was performed on testing samples in accordance with NQA-1-2000 and the QA requirements of the DOE/RL-96-68, *Hanford Analytical Services Quality Assurance Requirements Documents* (HASQARD), Volumes 1 and 4, latest revision, or equivalent document(s). Analytical methods and associated QA and quality control (QC) limits are specified in the HASQARD, and were applied to the analytical work under this program. For analytes and methods not covered in HASQARD, the approach to QA and QC was similar to the general approach outlined in HASQARD.

The analytical work for rheological, particle size distribution (PSD), density, and wt% solids were conducted under the WTPSP QA Program and were categorized as technology level “Applied Research” in accordance with the WTPSP QA Program.

Simulant development for small- and full-scale testing that was conducted at PNNL under the WTPSP QA Program and categorized as technology level “Applied Research” in accordance with the WTPSP QA Program.

## **1.5 Report Organization**

This report discusses the characteristics of the MADC-4 non-Newtonian simulant as described in the following sections:

- Section 2.0: Describes simulant preparation and analysis methods used to conduct the non-Newtonian simulant development.
- Section 3.0: Presents non-Newtonian simulant testing and results, including the recommended recipe and remaining technical uncertainties.
- Section 4.0: Describes special topics in the recommended simulant performance, such as dilution behavior, temperature dependence, and wet-sieving.
- Section 5.0: Contains a summary of the non-Newtonian simulant and conclusions.



## 2.0 Simulant Preparation and Characterization Methods

This section discusses how the simulant samples were prepared (Section 2.1) and the methods used for characterization of the physical properties (Section 2.2). The preprocessing of the raw LDSP is discussed here also.

### 2.1 Simulant Preparation

Simulant slurries were generated using the raw materials listed in Table 2.1, with all the simulant slurries prepared using RCW. In order to obtain correctly sized particles ( $> 100 \mu\text{m}$ ) for the LDSP, additional preparation of the basalt and Zirox was required. The basalt material as-received from the vendor was sieved to obtain the desired particle size range as per Slaathaug (2016). The material was dry sieved using a Ro-tap sieve shaker; material less than 50 mesh ( $300 \mu\text{m}$ ) and above 45 mesh ( $355 \mu\text{m}$ ) was removed from the raw material. Recovery in the particle size range of interest was approximately 11 wt%. Similarly, the Zirox was sieve cut to remove particles smaller than  $\sim 100 \mu\text{m}$  using the Ro-tap sieve shaker and a 140-mesh ( $106\text{-}\mu\text{m}$ ) sieve. Recovery for the Zirox in this particle size range was approximately 61% by mass.

PSDs of the sieved components of the LDSP were measured to evaluate the sieve sizing and are shown in Figure 2.1. Sieving was intended to remove particles less than  $300 \mu\text{m}$  and greater than  $355 \mu\text{m}$  for the basalt and particles less than  $\sim 100 \mu\text{m}$  for the Zirox. Evaluation of the PSDs for the sieved materials finds that the basalt solids still contain a significant fraction of particles above  $355 \mu\text{m}$ . Similarly, the Zirox solids still contain a small fraction below  $100 \mu\text{m}$ . It should be noted that the differences between the size distributions measured by laser diffraction and those resulting from the combination of sieve cuts used are expected and can be attributed to several factors. Sieving can be more or less effective depending on the morphology of the particles and their size relative to the sieve mesh selected and sieve particle loading. Elongated particles can pass through the sieve mesh, resulting in larger particles being observed when particle size is measured using laser diffraction such as the Malvern MS2000. Blinding can occur, resulting in the inclusion of particles that would normally be cut by the sieving process. Furthermore, laser diffraction measurements typically yield an artificial broadening of the PSD as a result of smoothing factors in the algorithms used to convert the measured light scattering patterns to PSDs (see Appendix G of Wells et al. 2011).

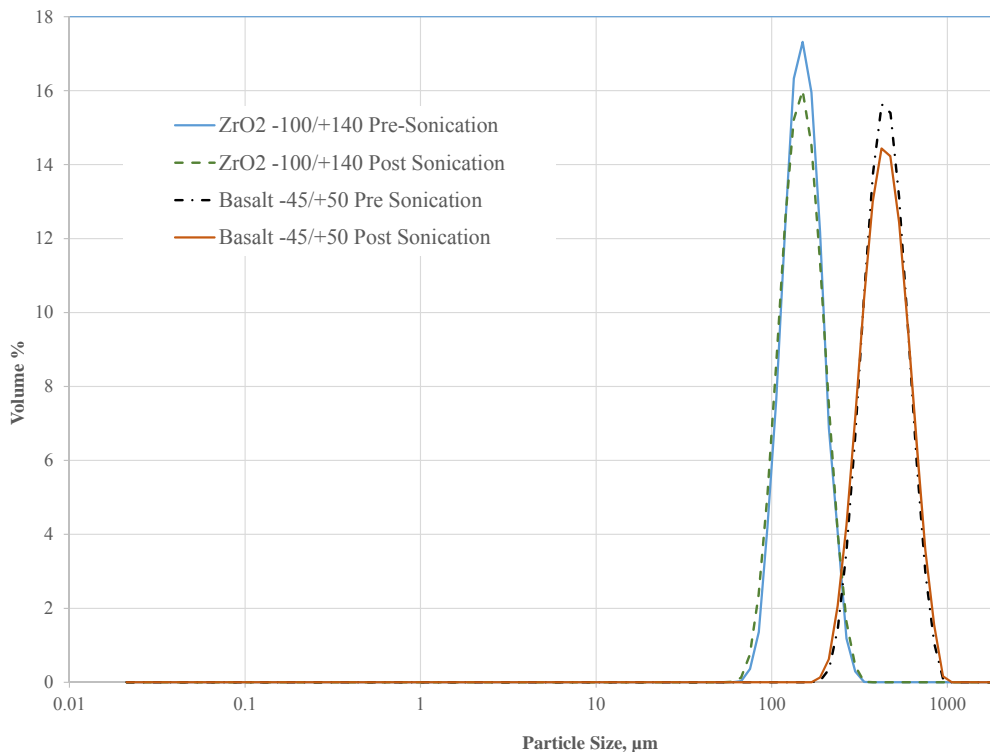


**Figure 2.1.** Particle size distribution of sieved components of the LDSP, pre-sonication and post-sonication.

Unless otherwise stated, sodium chloride was dissolved in RCW prior to the addition of clay powders. Bentonite clay powder was always added first to the salt water solution as a pre-mixed 1:1 blend by weight ratio with kaolin. The simulant was mixed by hand shaking the capped container, and once the kaolin/bentonite powder was fully wet, the remaining components were added, excluding the biocide, in the following order: the remaining kaolin, Zirox, and finally the basalt. Bentonite was added as a kaolin/bentonite blend to prevent bentonite, a gelling clay, from forming gelatinous clumps that can take hours to days to dissipate depending on the batch size of slurry made. Samples were then put on a mechanical shaker for an initial mixing period of a minimum of 12 hours, after which biocide was added at a dose rate of ~100 ppmv. The simulant slurries were allowed to sit for approximately 1 week, during which they were periodically hand shaken. After the initial hydration period, physical properties were analyzed.

An assessment of aging effects on selected simulant samples (discussed in Section 3.3.2) was performed by reanalyzing the rheology of sample(s) of interest after additional time had elapsed. In cases where rheology of a sample was measured at multiple times (ages), the parent sample was sub-sampled to perform the measurement. Replicate samples were made of the final selected simulant formulation, both with and without added LDSP. Initial samples made for all target formulations were 200 mL. Select

formulations were scaled up to 400 mL, and it was intended to scale up to larger volumes, but time constraints did not allow for that scope (described in PP-WTPSP-145, Rev 0.0<sup>1</sup>) to be executed.

**Table 2.1.** MADC-4 simulant component information.

Component	Supplier/Product ID	Sieve Cut Mesh (microns)	Particle Size, d(50) (microns)	Particle Density (g/mL)	Moisture Content (%)
Kaolin	Edgar Minerals, EPK	NA	NM	2.65 <sup>(a)</sup>	1.78
Bentonite	WYO-Ben Inc., Big Horn 200	NA	NM	2.55 <sup>(a)</sup>	6.36
Basalt	Dresser Trap Rock, Inc., Manufactured Sand #40 Product 812 (sieved to pass through a 45 mesh sieve and retained on a 50 mesh sieve)	-45/+50 (-350 µm/+300 µm)	442	3.00	NM <sup>(b)</sup>
Zirconium oxide (Zirox)	Washington Mills (Durazon) Zirox -100/+170 (sieved and retained on a 140 mesh)	-100/+140 -150 µm/+106 µm	149	5.78	NM <sup>(b)</sup>
NaCl	Fisher Scientific, S640-10, USP/FCC Granular	NA	NA	2.16 <sup>(a)</sup>	NM <sup>(b)</sup>
Biocide	U.S Water Services, Biotrol-509 (5wt% 2,2-dibromo-3-nitrilpropionamide, DBNPA)	NA	NA	NA	NM

NA = not applicable; NM = not measured.  
(a) Nominal values taken from product information sheets, assumed to be dry solid density.  
(b) Assumed to be negligible.

## 2.2 Characterization Methods

Slurry samples were characterized for physical and rheological properties including PSD, bulk density, solids content, yield stress, and consistency. Sample analyses were performed according to procedures RPL-COLLOID-02, Rev. 2, *Measurement of Physical and Rheological Properties of Solutions, Slurries and Sludges*; OP-WTPSP-004, Rev. 1, *Operation of the Mettler Moisture Analyzer*; and OP-WTPSP-003, Rev. 1, *Size Analysis Using Malvern MS2000*.

### 2.2.1 Rheology

Rheological characterizations were performed in accordance with RPL-COLLOID-02, Rev. 2.0, using a Haake RS600 rheometer operated with RheoWin Pro 4.41.0019 Software (Thermo Electron Corporation). The RS600 rheometer is equipped with a low-inertia torque motor and a coaxial cylinder measurement

<sup>1</sup> Burns, CA. 2016. *Non-Newtonian Simulants for the Standard High Solids Vessel Design*. PP-WTPSP-145, Rev 0.0, Pacific Northwest National Laboratory, Richland, WA.

geometry. The drive shaft of the motor is centered by an air bearing that ensures an almost frictionless transmission of the applied torque to the sample. Unless specified otherwise, all rheological analyses were conducted at 25°C. Samples were gently shaken by hand to ensure complete mixing before introducing them into the measuring device. Before any flow curves were measured, a pre-shear at a constant 200 s<sup>-1</sup> rate for 3 min was performed on all simulant samples. Flow curves were obtained by shearing the sample at a controlled rate from zero to 1000 s<sup>-1</sup> for 5 min, holding constant at 1000 s<sup>-1</sup> for 1 min, and then shearing at a controlled rate from 1000 s<sup>-1</sup> to zero for 5 min. This procedure was performed three times, and the second measurement was used for data analysis. For all values reported, the down ramp from 800 to 250 s<sup>-1</sup> was used to evaluate the flow curves.

Understanding and interpreting the flow curves is critical to assessing the rheology of the non-Newtonian simulants. For these measurements, non-elastic flow of non-Newtonian materials is characterized with rotational viscometry. The goal of rotational viscometry is measurement of a material's flow curve, which describes the shear stress response,  $\tau$ , as a function of applied shear rate,  $\dot{\gamma}$  (also called the rate-of-strain). The result of a flow curve measurement is a set of  $\tau$  versus  $\dot{\gamma}$  measurements, which are called flow curve data. Flow curve data can be interpreted with several constitutive equations that relate viscous stress to shear rate. Such analysis allows the flow behavior over a broad range of conditions to be described with just a few rheological descriptors (e.g., viscosity, yield stress, consistency, and flow index).

Flow curves were measured using a concentric cylinder rotational viscometer operated in controlled rate mode. These types of viscometers operate by placing a given volume of test sample into a measurement cup of known geometry. A cylindrical rotor attached to a torque sensor is lowered into the sample until the slurry is even with, but does not cover, the top of the rotor. For a given concentric cylinder geometry, both the radius and the height of the rotor are known such that the gap distance between cup and rotor and surface area of fluid contact can be determined. In addition, the top and bottom of the rotor have recessed surfaces such that the fluid only contacts the radial surfaces of the rotor. A filled rotor-in-cup test geometry is shown in Figure 2.2. Fluid flow properties of a sample are determined by spinning the rotor at a known rotational speed,  $\Omega$ , and measuring the resisting torque,  $M$ , acting on the rotor. Because fluid only contacts the rotor on the radial surfaces of rotation, all of the force resisting steady-state rotation can be ascribed to shearing of the fluid in the cup-rotor gap. Assuming an isotropic fluid and cup and rotor dimensions as shown in Figure 2.2., the torque acting on the rotor can be directly related to the shear stress at the rotor using the equation

$$\tau = \frac{M}{2\pi HR_j^2} \quad (2.1)$$

Shear stress is measured in units of force per area [N/m<sup>2</sup>]. Calculation of the fluid shear rate at the rotor is complicated by the fact that shear rate depends both on the measurement system geometry and the fluid rheological properties. For the simplest fluids (i.e., Newtonian fluids) the shear rate of the fluid at the rotor can be calculated given the geometry of the cup rotor shear (see Figure 2.2.) by using the equation

$$\dot{\gamma} = \left( \frac{2R_o^2}{R_o^2 - R_i^2} \right) \Omega \quad (2.2)$$

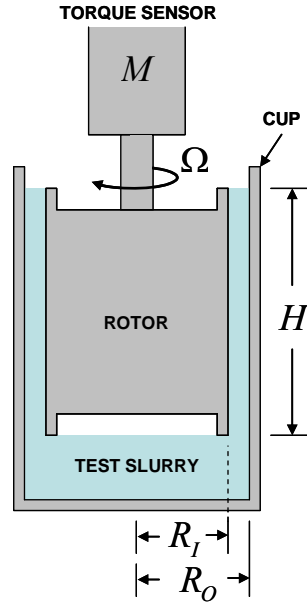


**Figure 2.2.** Rotor and cup geometry used in rotational viscometry testing used for simulant development.

Here, shear rate has units of inverse seconds [1/s]. Calculation of shear rate for materials showing more complex shear stress versus shear rate behavior (i.e., non-Newtonian fluids) requires input of flow curve parameters (e.g., yield stress and degree of shear-thinning or shear-thickening). Typically, because the required input parameters are not known prior to measurement, this requirement is circumvented by using a cup and rotor system with a small gap (~1 mm) such that shear rate effects introduced by fluid properties are minimized. For these systems, Eq. (2.3) provides an accurate determination of shear rate for non-Newtonian materials.

The resistance of a fluid to flow can also be described in terms of the fluid's apparent viscosity,  $\eta_{app}$ , which is defined as the ratio of the shear stress to shear rate:

$$\eta_{app} = \frac{\tau}{\dot{\gamma}} \quad (2.3)$$

The units of apparent viscosity are Pa·s; however, viscosity is typically reported in units of centipoise (cP; where 1 cP = 1 mPa·s).

As stated above, flow curve data can be interpreted with several constitutive equations (i.e., flow curves), allowing characterization of that data with just a few rheological descriptors. The behaviors of the slurries have been described by the Bingham plastic flow curve equation for the MADC-4 simulant.

Bingham plastics are fluids that show finite yield points. This stress (i.e., the yield stress) must be exceeded before these types of materials flow. Once flow is initiated, the stress response of the material is linear over the rest of the shear rate range. Bingham plastics are described by the expression

$$\tau = \tau_o^B + k_B \dot{\gamma} \quad (2.4)$$

where  $\tau_o^B$  is the Bingham yield index (or stress) and  $k_B$  is the Bingham consistency index.

Concentrated slurries can show complex flow curve phenomena, including both time-independent and time-dependent behaviors. Figure 2.3 outlines flow behaviors typical of sludge materials. With respect to time-independent behaviors, yield stress materials can be classified by changes in the slope of the equilibrium flow curve after material yield (see Figure 2.3a). Materials that show increasing slope with applied shear rate are considered “shear-thickening” yield materials, whereas materials with decreasing slope are considered to be “shear thinning.” Materials with constant slope after yield are referred to as Bingham plastics. These types of flow behavior are time-independent and do not depend on the direction the flow curve is being measured (i.e., the stress response is the same when measured with increasing shear rate or decreasing shear rate). As such, time-independent changes are reversible.

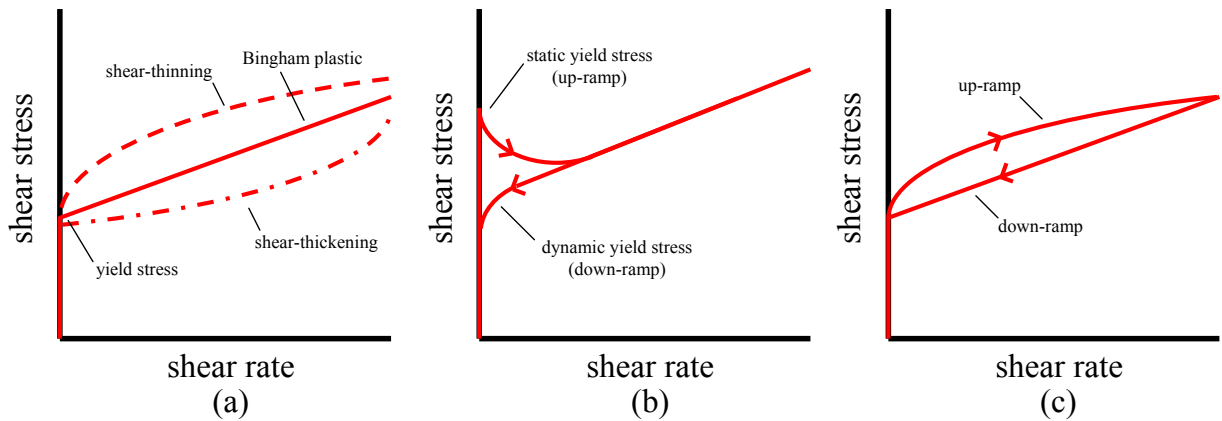


**Figure 2.3.** Summary of flow curve behaviors typically observed for concentrated slurries, including (a) common time-independent behaviors, (b) static and dynamic yield stress, and (c) flow-curve hysteresis.

Time-dependent flow curve phenomena refer to immediately irreversible (i.e., either short-term or permanent) changes in the stress response of a material. These changes can be caused by the application of shear or may simply occur over time. Time-dependent phenomena can be attributed to breakage of slurry structure, settling of dispersed solids, or changes in the chemistry of slurry components. As shown in Figure 2.3b and Figure 2.3c, time-dependent phenomena can manifest as the different static and dynamic slurry yield stresses and as flow curve hysteresis.

## 2.2.2 Density

Bulk density of the slurry samples was measured using certified glass pycnometers in accordance with RPL-COLLOID-02, Rev 2.0. All density measurements were performed at ambient temperature. Daily balance checks were performed with calibrated check weights when the balance was in use. After the balance performance check, the tare weight of the pycnometer to be used was obtained and recorded. The pycnometer was then filled with the simulant fluid to be measured. The gross weight of the pycnometer containing the simulant fluid was obtained. The net weight of the simulant fluid was calculated by subtracting the pycnometer tare weight from the gross weight of the pycnometer containing the simulant. The bulk density of the simulant fluid was calculated using Eq. (2.5). Unless specified otherwise, all density measurements were carried out at room temperature. Room temperature associated with each

density measurement was measured using a calibrated thermocouple and recorded with the density measurement data, typical temperatures ranged from 22 to 25 °C.

$$\rho = \frac{M}{V} \quad (2.5)$$

where  $\rho$  is bulk density (g/mL),  $M$  is net weight of the simulant fluid (g), and  $V$  is volume of the simulant fluid (mL).

### 2.2.3 Particle Size Analysis

Particle size characterization was accomplished using a Mastersizer 2000 (Malvern Instruments, Inc., Southborough, Massachusetts) with a Hydro G wet dispersion accessory (equipped with a continuously variable and independent pump, stirrer, and ultrasound). The Mastersizer 2000 has a nominal size measurement range of 0.02 to 2000  $\mu\text{m}$ . The actual range is dependent on the accessory and the properties of the solids being analyzed. When coupled with the Hydro G wet dispersion accessory, the nominal measuring range is 0.02 to 2000  $\mu\text{m}$  (this is dependent on material density). Table 2.2 provides a summary of basic information regarding the analyzer and accessory. A NIST-traceable particle size standard is used to evaluate the performance of the particle size analyzer in accordance with OP-WTPSP-003, Rev. 1.0.

**Table 2.2.** Summary of Malvern Mastersizer 2000 instrument information.

Analyzer:	Malvern Mastersizer 2000 (Serial No. MAL 1019545)
Measurement principle:	Laser diffraction (Mie scattering)
Analyzer accessory:	Hydro G, 800 mL capacity
Measurement range:	0.02 to 2000 $\mu\text{m}$ nominal
Type:	Flow cell system with continuously variable and independent pump, overhead stirrer, and ultrasound (20 watt full power)

Approximately 1 to 2 g of dry material was diluted with tap water in the Hydro G dispersion unit with pump and stirrer speed set typically at 2500 and 1000 rpm, respectively, for 60 s before making the particle size measurements. Appropriate dilutions were determined by the amount of light passing through the diluted material (obscuration), which was measured by the particle size analyzer. Samples were analyzed on the same aliquot initially without sonication and then during sonication (100%, 20 W) after an initial sonication period of 60 s and also post-sonication.

All PSD data given in this report are averages of three measurements taken from one aliquot for each measurement condition, i.e., three measurements prior to sonication, three during sonication, and three post-sonication.

### 2.2.4 Solids Content

The total solids content of slurry samples by weight was determined using a Mettler-Toledo Halogen Moisture analyzer (Model HR83, Serial No. 1129192189) in accordance with OP-WTPSP-004, Rev. 1, *Operation of the Mettler Moisture Analyzer*. Approximately 5 to 10 g of slurry material was introduced

into the moisture analyzer and a preprogrammed drying program was run. The program consisted of an initial hold period of 30 min at 95 °C, and then a second temperature of 105 °C was used to complete the drying process. The criterion for ending the program was set to a mean weight loss of 1 mg over a 140 s period. The results were recorded as dry content (i.e., total solids content) by the moisture analyzer; the definition of this result is given by Eq. (2.6).

$$\text{Dry Content} = \frac{\text{dry weight}}{\text{wet weight}} \times 100\% \quad (2.6)$$

## 3.0 Non-Newtonian Simulant: Testing and Results

This section presents the process of iterating to the recommended non-Newtonian simulant. This includes the initial parametric study used to encompass the target rheology (Section 3.1), refinements to the simulant formulation based on the results of the parametric study (Section 3.2), a discussion of the recommended simulant and its preparation and aging behavior (Section 3.3), and a description of typical rheological behavior of the recommended simulant (Section 3.4). The final two sections provide a short discussion of technical uncertainties with respect to the process of selecting the recommended simulant (Section 3.5) and a note on the dry basis of the simulant (Section 3.6).

### 3.1 Initial Parametric Study

The initial parametric study was concerned with focusing on the composition of clay solids and salt concentrations that had rheological parameters near the target range. Since the focus of the non-Newtonian simulant development is primarily concerned with meeting a rheology target, the development process was otherwise unconstrained, i.e., the density and composition of the carrier fluid (clay slurry) did not have defined target values and the constituents making up the LDSP were already fully defined. Thus, the parametric study made an array of samples to bound the target rheology with the intention of refining to a composition that was closer to the target. Unless noted, samples were prepared with the LDSP incorporated in the appropriate amount.

The initial suite of samples was selected based on a combination of two factors:

1. PNNL's historical experience with kaolin/bentonite clay slurries used in experimental measurements; for examples see Bontha et al. (2007), Daniel et al. (2013), or Schonewill et al. (2013, 2015). Most PNNL references attribute the origination of this clay formulation to Rassat et al. (2003).
2. An extensive set of scoping samples that were prepared (unpublished, For Information Only) prior to executing this study.

Table 3.1 lists the array of initial samples that were prepared, presented with their *nominal, solids-free* compositions.<sup>1</sup> To convert from the nominal carrier fluid composition to actual compositions, recall that the clay solids in all the samples are in an 80%/20% kaolin/bentonite ratio (by mass) and there is inherent moisture in the clay solids (~2% for kaolin and ~6% for bentonite, by mass). The LDSP (Zirox and basalt) were added at a fixed mass so the actual mass fraction will vary slightly from sample to sample. For convenience, each sample was given a single identifier beginning from NN-001 and incrementing by one for each unique sample. Note the implication of this convention is that each identifier refers to a unique sample and not necessarily a unique simulant composition.

---

<sup>1</sup> To further clarify: The nominal, solid-free clay solids are the proportion of those solids that would be added of the as-received material to make up the non-Newtonian carrier fluid. They are not on a dry basis; taking account of the moisture content of the clay solids and the LDSP will yield the "true" solids concentration (dry basis, entire simulant mixture) of the clay solids in each sample.

**Table 3.1.** Composition of initial parametric samples.

Sample ID	RCW (wt%)	Clay (wt%)	Kaolin (wt%)	Bentonite (wt%)	NaCl (wt%)	Theoretical Density <sup>(a)</sup> (g/mL)	Rheology Measurement Time <sup>(b)</sup> (days)
NN-001	66.00	34.0	27.2	6.8	0.00	1.256 [1.289]	6.92
NN-002	65.00	35.0	28.0	7.0	0.00	1.265 [1.299]	6.89
NN-003	64.00	36.0	28.8	7.2	0.00	1.275 [1.309]	6.83
NN-004	63.00	37.0	29.6	7.4	0.00	1.285 [1.318]	6.79
NN-005	65.90	34.0	27.2	6.8	0.10	1.257 [1.291]	5.81
NN-006	64.90	35.0	28.0	7.0	0.10	1.267 [1.301]	5.76
NN-007	63.90	36.0	28.8	7.2	0.10	1.277 [1.310]	5.64
NN-008	62.90	37.0	29.6	7.4	0.10	1.287 [1.320]	5.59
NN-009	65.80	34.0	27.2	6.8	0.20	1.259 [1.292]	6.85
NN-010	64.80	35.0	28.0	7.0	0.20	1.268 [1.302]	6.89
NN-011	63.80	36.0	28.8	7.2	0.20	1.278 [1.311]	6.92
NN-012	62.80	37.0	29.6	7.4	0.20	1.288 [1.321]	6.95
NN-013	65.95	34.0	27.2	6.8	0.05	1.257 [1.290]	7.81
NN-014	64.95	35.0	28.0	7.0	0.05	1.267 [1.300]	7.90
NN-015	63.95	36.0	28.8	7.2	0.05	1.276 [1.310]	7.93
NN-016	62.95	37.0	29.6	7.4	0.05	1.286 [1.320]	7.96

- (a) The following masses of Zirox and basalt were added to each 200 mL sample: 8.16 g of Zirox and 0.66 g of basalt. Two values for the theoretical densities are given in this column: density of the carrier fluid only, i.e., the clay slurry, and [density of the entire sample, i.e., including LDSP].
- (b) This is the elapsed time (in days) from when the sample was initially prepared (all materials mixed together) to when the measurement was made.

Each sample in Table 3.1 was prepared as described in Section 2.1 and then allowed to age at ambient conditions until the rheology was measured. The measurement time (in days) is given in Table 3.1 from when the sample was prepared. As these samples were for the purpose of refining the simulant recipe, the rheology of the samples was not tracked with sample age, and the majority of these samples were only measured a single time. The Bingham rheology parameters for the 16 samples are plotted in Figure 3.1; samples with common NaCl concentrations are grouped together. In general, it was expected that increasing NaCl concentration for the same clay concentration should increase the yield stress, and this is what is observed (see Figure 3.2). To a lesser extent, the same effect is observed with the consistency.

The most important observation from Figure 3.2 is the location of the rheological parameter targets in relation to the provided data. In Figure 3.2, both salt concentrations at 35% clay had measured yield stresses below the target; likewise, both salt concentrations at 37% clay were above the target. Based on this information, it was expected that the target parameters should be met with a non-Newtonian simulant that had a nominal clay solids concentration  $35.5\% < c_{\text{clay}} < 36.5\%$  and a salt concentration  $0.05\% < c_{\text{NaCl}} < 0.1\%$ . The next phase of sample preparation sought to refine the recipe in those concentration regions based on interpolation from the initial parametric data.

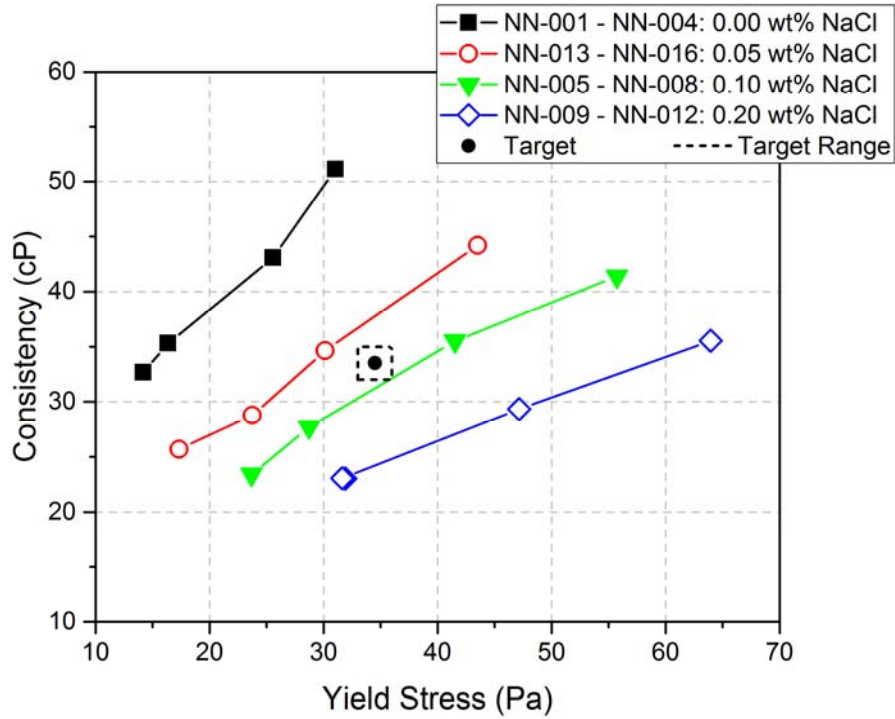


**Figure 3.1.** Measured rheological parameters of the initial parametric samples compared to the rheological parameter targets (shown as a black circle surrounded by a dotted line).

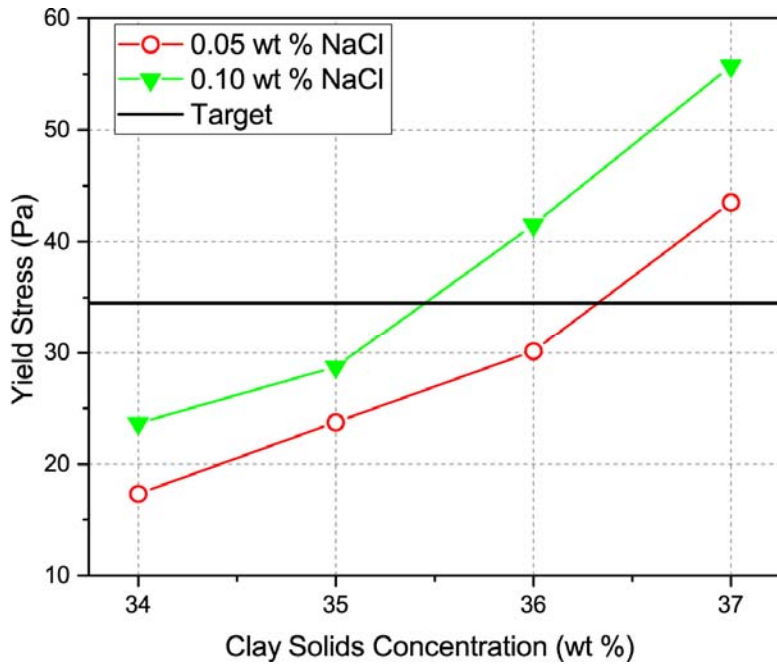


**Figure 3.2.** Bingham yield stress versus nominal clay solids concentration for parametric samples NN-005 through NN-008 (0.10 wt%) and NN-013 through NN-016 (0.05 wt%). The target yield stress (black line) is shown for reference.

### 3.2 Refinement from Parametric Data

To refine the carrier fluid to be closer to the target rheological parameters, the data was used to interpolate to a composition that was projected to obtain the target value (or at least fall within the target range). The interpolated composition (the “best-guess” recipe) was prepared in triplicate along with samples containing small perturbations around that composition. The refined simulant compositions that were prepared are shown in Table 3.2. The best-guess composition is given by NN-017, NN-018, and NN-019. The perturbations are  $\pm 0.2$  wt% on the clay solids concentration (NN-020, NN-021) or  $\pm 0.01$  wt% on the NaCl concentration (NN-022, NN-023). The expectation was if the “best-guess” recipe was not within the target range, either one of the perturbations would be or the range of information from the perturbation samples would indicate further adjustments to the composition. The “best-guess” recipe was prepared in triplicate to assess the variability between samples in measured Bingham rheological parameters.

**Table 3.2.** Composition of refined simulant samples.

Sample ID	RCW (wt%)	Clay (wt%)	Kaolin (wt%)	Bentonite (wt%)	NaCl (wt%)	Theoretical Density <sup>(a)</sup> (g/mL)	Rheology Measurement Time <sup>(b)</sup> (days)
NN-017	64.22	35.7	28.56	7.14	0.08	1.274 [1.307]	7.81
NN-018	64.22	35.7	28.56	7.14	0.08	1.274 [1.307]	7.84
NN-019	64.22	35.7	28.56	7.14	0.08	1.274 [1.307]	8.02
NN-020	64.42	35.5	28.40	7.10	0.08	1.272 [1.305]	7.94
NN-021	64.02	35.9	28.72	7.18	0.08	1.276 [1.309]	7.87
NN-022	64.21	35.7	28.56	7.14	0.09	1.274 [1.307]	7.91
NN-023	64.23	35.7	28.56	7.14	0.07	1.274 [1.307]	7.98

- (a) The following masses of Zirox and basalt were added to each 200 mL sample: 8.16 g of Zirox and 0.66 g of basalt. Two values for the theoretical densities are given in this column: density of the carrier fluid only, i.e., the clay slurry, and [density of the entire sample, i.e., including LDSP].
- (b) This is the elapsed time (in days) from when the sample was initially prepared (all materials mixed together) and when the measurement was made.

The Bingham parameters measured for the samples in Table 3.2 are shown in Figure 3.3. For reference, the target Bingham parameters and the target range are shown. On average, the “best-guess” composition samples were measured to have a yield stress of 32.3 Pa and a consistency of 33.3 cP, and this is very near the target range. However, only one of the three triplicate samples was within the range, and as Figure 3.3 shows, the spread in these three samples was  $\sim 3$  units in both parameters. Given that the yield stress tends to decrease slightly as the slurry ages, a composition that gave a slightly higher yield stress initially was preferred to avoid potentially sliding out of the target range as the simulant ages.

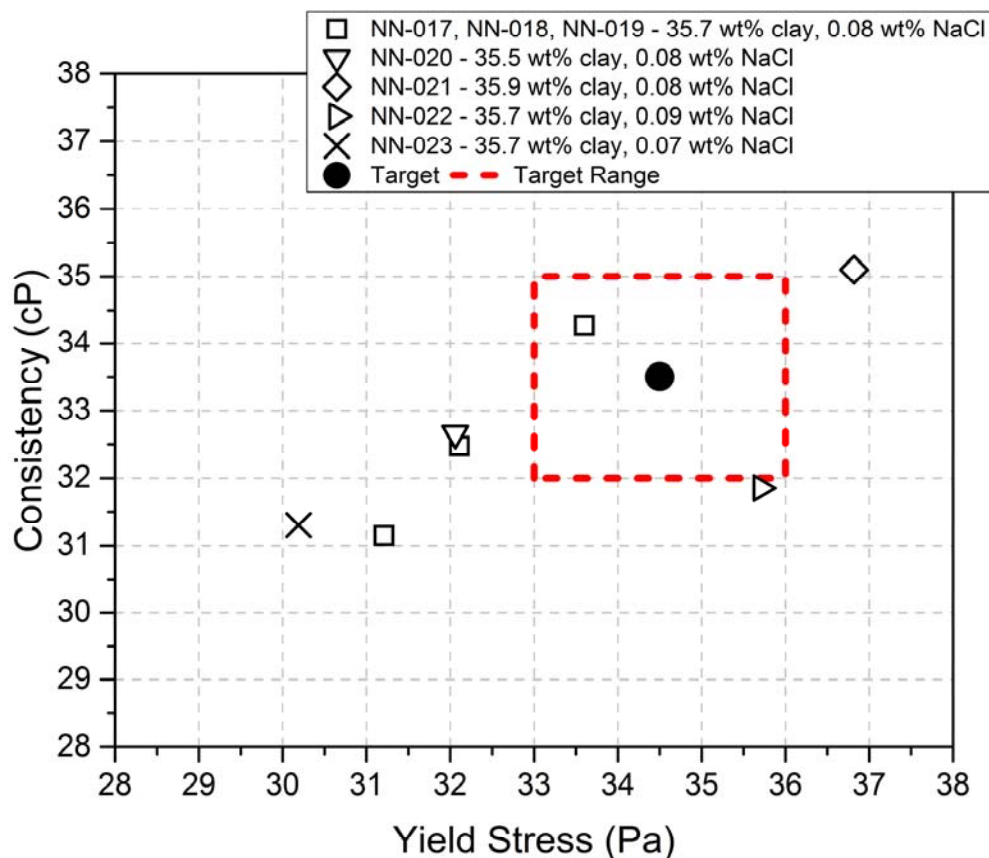


**Figure 3.3.** Bingham rheology parameters for refined simulant compositions. Note that the “best estimate” sample was prepared in triplicate (open squares).

### 3.3 Selection of the Recommended Simulant

Based on the data presented in Section 3.2, the formulation of NN-022 was selected for further investigation, as it was nearly within the target parameters range upon the first assessment of the rheological parameters (Figure 3.3). In addition, it also had a yield stress that was on the higher side of the target range rather than the lower side. To probe the repeatability of the sample properties, a duplicate of the NN-022 sample was prepared (NN-026) along with a couple perturbations (NN-024, NN-025) of the new target formulation at a larger sample volume, e.g., 400 mL. These formulations are given in Table 3.3. The rheology of these samples was measured before the typical aging period of ~7 days (at around 3 days), and so the measured yield stress on all the samples was > 40 Pa<sup>1</sup>. However, the NN-026 sample met the consistency target and so it was expected the yield stress would drop near or into the target range as the sample continued to age (later confirmed by measurement<sup>2</sup>).

<sup>1</sup> Bingham parameters measured at approximately 3 days from preparation were: NN-024 – 43.8 Pa / 34.4 cP, NN-025 – 41.0 Pa / 33.1 cP, and NN-026 – 43.4 Pa / 33.5 cP.

<sup>2</sup> At approximately 12 days from preparation for NN-026, the measured Bingham parameters were a yield stress of 37.3 Pa and a consistency of 34.0 cP; at 19 days the yield stress was 33.4 Pa.

The three samples in Table 3.3 each had Bingham parameters that were very similar, and it is possible that any of those three formulations could be used to achieve the target rheological parameters. The data needed to confirm this possibility have not been collected, i.e., the evolution of rheology with time for samples NN-024 and NN-025 was not monitored. Based on this preliminary sample data, the NN-022 formulation was selected as the “best”<sup>1</sup> recipe to recommend. As kaolin/bentonite clay slurries are known to experience shifts in Bingham parameters as the suspension ages, NN-022 and NN-026 were measured periodically to assess the stability of the rheological parameters. A more extensive discussion of the aging observed in these samples is provided in Section 3.3.2.

**Table 3.3.** Composition of samples NN-024, NN-025, and NN-026.

Sample ID	RCW (wt%)	Clay (wt%)	Kaolin (wt%)	Bentonite (wt%)	NaCl (wt%)	Theoretical Density <sup>(a)</sup> (g/mL)	Rheology Measurement Time <sup>(b)</sup> (days)
NN-024	64.22	35.8	28.64	7.16	0.085	1.275 [1.308]	2.83
NN-025	64.22	35.5	28.40	7.10	0.085	1.272 [1.305]	2.87
NN-026	64.22	35.7	28.56	7.14	0.090	1.274 [1.307]	2.91

- (a) The following masses of Zirox and basalt were added to each 400 mL sample: 16.33 g of Zirox and 1.31 g of basalt. Two values for the theoretical densities are given in this column: density of the carrier fluid only, i.e., clay slurry, and [density of the entire sample, i.e., including LDSP].
- (b) This is the elapsed time (in days) from when the sample was initially prepared (all materials mixed together) and when the measurement was made.

### 3.3.1 Effect of Preparation Sequencing

The preparation of the previously described simulants NN-001 to NN-026 had all been performed in the same manner, i.e., mixing all the components together at the same time. Before confirming the viability of the “best” recipe, it was important to assess if the mixing sequence of the simulant components affected (in any significant way) the rheological parameters. If the Bingham parameters are invariant to the mixing sequence, this affords additional flexibility when mixing the simulant at larger scale. If, however, the rheology is sequence-dependent, then it would be important to help identify the sequences or steps that were critical to obtaining the necessary rheological behavior.

The rheological measurements on the majority of the samples had also exhibited an unexpected amount of hysteresis, and it was suspected (but unknown) that the hysteresis could be due to either the added solids (Zirox, basalt) or the presence of the NaCl in the carrier phase. To probe both of these potential causes further, the simulant formulation representing the “best” recipe was prepared in six unique sequences to elucidate the impact. The sequence variants are explained in Table 3.4. Note that the variants only alter the preparation sequence, and after the appropriate solids are added, samples NN-027, NN-028, NN-030, and NN-031 are all identical in composition (and also are the same as previous “best” recipe samples NN-022 and NN-026). Samples NN-029 and NN-032, which do not contain the LDSP, were prepared to see

<sup>1</sup> The target recipe is consistently referred to as the “best” recipe in this report; it is enclosed in quotation marks to signify that it is not the only possible formulation that would result in the target Bingham parameters.

the effect (if any) that the LDSP had on the measured rheology. They still share the same carrier fluid composition with the other four samples.

**Table 3.4.** Sequencing variants of “best” recipe NN-022.

400 mL Sample Set	Sample ID	Components Initially Mixed	Component(s) Added After Hydration Period	Hydration Period (days)	Rheology Measurement Time <sup>(a)</sup> (days)	Notes
LDSP Triad	NN-027	All	N/A	N/A	7.84 <sup>(b)</sup>	Identical to samples NN-022 and NN-026.
	NN-028	Clay, RCW, NaCl	Zirox, basalt	~8	9.79 <sup>(b, c)</sup>	NN-027 with LDSP added later.
	NN-029	Clay, RCW, NaCl	N/A	N/A	7.94 <sup>(b)</sup>	NN-027 with no LDSP added.
Salt Triad	NN-030	Clay, RCW, Zirox, basalt	NaCl	~10	11.89 <sup>(d)</sup>	NN-027 with NaCl added later.
	NN-031	Clay, RCW	NaCl, Zirox, basalt	~10	11.92 <sup>(e)</sup>	NN-027 with NaCl and LDSP added later.
	NN-032	Clay, RCW	NaCl	~10	11.96 <sup>(d)</sup>	NN-027 with NaCl added later and no LDSP.

- (a) This is the elapsed time (in days) from when the sample was initially prepared (all materials mixed together) to when the measurement was made.
- (b) Rheology data measured at ~11 days (preferable for comparison because the elapsed times were the same) was removed from consideration in the analysis set due to a measurement shear range inconsistency.
- (c) First rheological measurement of the sample, ~2 days after solids addition.
- (d) A pre-NaCl addition rheological measurement was made at ~10 days.
- (e) First rheological measurement of the sample, ~2 days after salt and solids addition.

The measured rheological parameters are given in Table 3.5, along with the age, in days, of the simulant slurries. The sequencing in Table 3.4 can be cross-referenced with the data collection times to observe the effect of the mixing steps on rheological behavior. After evaluating the resultant data and associated rheograms, the following observations were made:

1. The presence of the LDSP, and when they were added to the sample, does not significantly affect the rheological parameters measured between samples of the same composition. The hysteresis does not appear to be caused by the presence or lack of presence of the LDSP, and it was still present in varying degrees in the LDSP Triad samples.
2. LDSP Triad samples began to stabilize and approach the yield stress and consistency target when the second reported measurement was performed (~3 weeks from preparation). Fluctuations in yield stress and consistency during the initial period were observed to be approximately 3 to 4 units. A time period of approximately 20 days was observed to mark a minimum in the measured Bingham parameters: compare, for example, the second and third measurements given in Table 3.5.
3. Salt Triad samples, before NaCl was added, had consistencies much greater than would be anticipated (> 40 cP). This is typically indicative of a clay solids concentration that is too large, as the primary

function of the NaCl is to stabilize the yield stress. These samples also had no or very little hysteresis in their rheograms.

4. After the addition of the salt, the yield stress increased dramatically (> 60 Pa) and the Salt Triad samples were well outside of the target range. The amplification of the yield stress upon salt addition is consistent with PNNL’s experimental experience using NaCl as an additive to already hydrated clay slurries (based on unpublished work).
5. Upon NaCl addition, the variation between Bingham parameters in the Salt Triad samples is small. However, some hysteresis was present in the rheograms post-NaCl addition. Based on this evidence, the presence of the salt appears to result in hysteresis in the simulant samples.

Based on these observations, it is critical that the “best” recipe be prepared with the NaCl fully dissolved in RCW (or some other water source) prior to the clay hydration period or the resultant slurry will have a yield stress > 60 Pa. The anecdotal evidence suggests that the combination of NaCl with the other simulant components creates a mixture where hysteresis will occur (whether LDSP are present or not) when rheological measurements are performed; this will add some uncertainty to the assessment of the “true” rheology of the non-Newtonian simulant. These measurements also indicate that some hydration time period is required, as the short-time behavior (< 15 days) is difficult to predict, and parameters fluctuate on the order (or greater) of the originally specified uncertainty ( $\pm 1.5$  units). Figure 3.4 illustrates an example of this from five similar samples (NN-022, NN-026, NN-027, NN-028, and NN-029) where the Bingham parameters were measured at approximately the same time.

**Table 3.5.** Measured Bingham parameters of sequencing variants.

Sample ID	First Rheology Measurement <sup>(a)</sup> (Pa / cP)	First Rheology Measurement Time <sup>(b)</sup> (days)	Second Rheology Measurement <sup>(a)</sup> (Pa / cP)	Second Rheology Measurement Time <sup>(b)</sup> (days)	Third Rheology Measurement <sup>(a)</sup> (Pa / cP)	Third Rheology Measurement Time <sup>(b)</sup> (days)
NN-027	35.4 / 33.4	7.84	31.1 / 33.3	20.93	36.5 / 36.7	45.83
NN-028	35.2 / 31.3	9.79	32.2 / 32.1	20.96	33.1 / 33.1	45.98
NN-029	33.3 / 30.5	7.94	34.4 / 33.1	21.00	37.7 / 34.6	45.93
NN-030	29.4 / 44.0	9.92	65.0 / 47.4	11.89	N/A	N/A
NN-031	N/A	N/A	63.9 / 47.5	11.92	N/A	N/A
NN-032	29.8 / 42.7	9.95	63.3 / 45.8	11.96	N/A	N/A

N/A = not available because data was not collected.

(a) The rheology measurements are given as yield stress (Pa) / consistency (cP) based on the second down ramp over the range 250 to 800 s<sup>-1</sup>.

(b) This is the elapsed time (in days) from when the sample was initially prepared (all materials mixed together) and when the measurement was made.

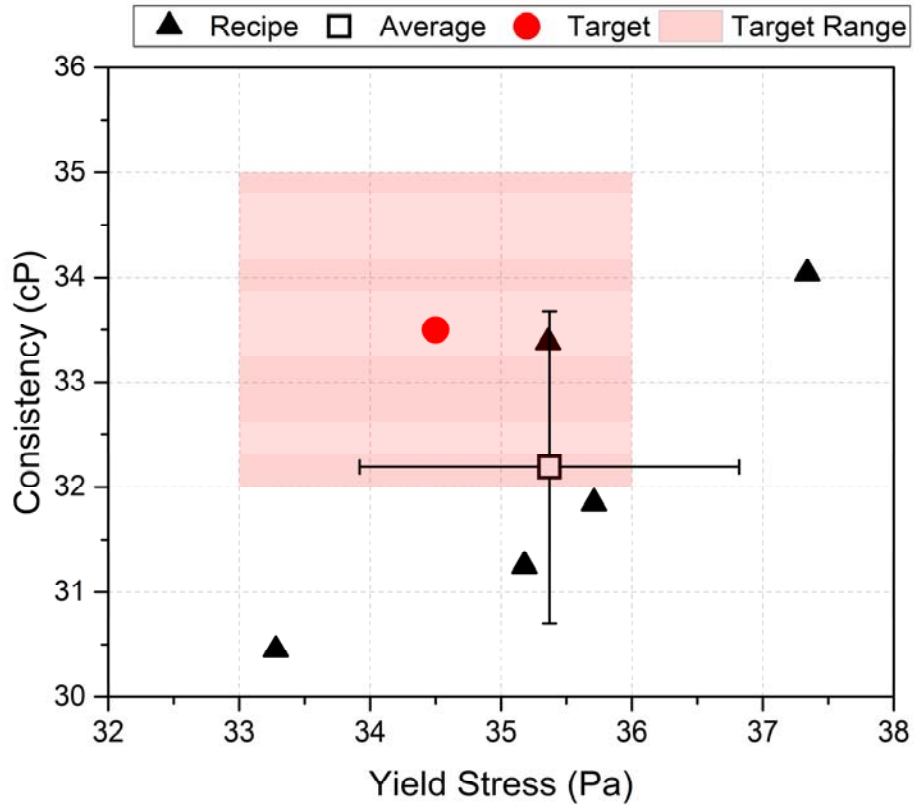


**Figure 3.4.** Rheological parameters of “best” recipe samples measured between 8 to 12 days. The data is included from samples NN-022, NN-026, NN-027, NN-028, and NN-029. The white square with error bars represents the mean of the five samples and the associated standard deviations of the mean.

Note that the data in Figure 3.4 demonstrates a range of approximately 4 units in the yield stress and 4 units in the consistency. The mean (average) value given in Figure 3.4 by the white square is within the target range, but the error bars (illustrating a standard deviation of the mean) stretch outside of the target range. As stated before, these samples have all aged for 12 days or less where the rheological behavior was found to have greater variability. The aging behavior of the “best” recipe was investigated further to ascertain if some stabilization in the Bingham parameters was achieved at longer times. This is described in the next section.

### 3.3.2 Effect of Sample Aging

Based on the data described so far, the “best” recipe was prepared eight separate times in samples NN-022 and NN-026 through NN-032. Recall that samples NN-030, NN-031, and NN-032, despite having the same final composition as the rest of the samples, exhibited very different rheological behavior, as discussed in Section 3.3.1 (i.e., the salt content was added following the initial hydration of the clay mixture). Thus, they were not included in the aging study described in this section. Also, it is worth mentioning that NN-029 data is included with the other four samples but it does not contain the LDSP like the rest of the samples. No significant differences were observed between the measured parameters

(or hysteresis) with or without LDSP, so NN-029 was tracked with the other samples in the aging study for completeness.

Each of the five samples with the “best” recipe composition was analyzed for Bingham parameters multiple times over an approximately 50-day period (determined from when the sample was first prepared). For each measurement, a sub-sample was collected from the parent sample to perform the rheology measurements, so over time the sample inventory was reduced. These samples were used to build an aggregate simulant rheological behavior with age. The aggregate behavior is generated by taking the discrete rheological data (a yield stress or consistency against a time since preparation) and averaging the data at the same time steps (in 2-day increments). Since not all data was taken at the same discrete points in time, the aggregation is performed by linearly interpolating between discrete data points. No extrapolation is performed with any data, so means near the end points of the aggregate data set include less sample measurements. In addition to the aggregate mean, standard deviations were generated with the same, interpolated data set. In Figure 3.5 and Figure 3.6, the aggregated yield stress and aggregated consistency with time are shown, respectively. The mean data is shown as a set of discrete step changes to more accurately portray how the data was combined, since the means are not based on continuous data sets. On each figure, the target range is shown as a shaded region, and the lower and upper limits represented by the dotted lines are the aggregate mean  $\pm$  one standard deviation.

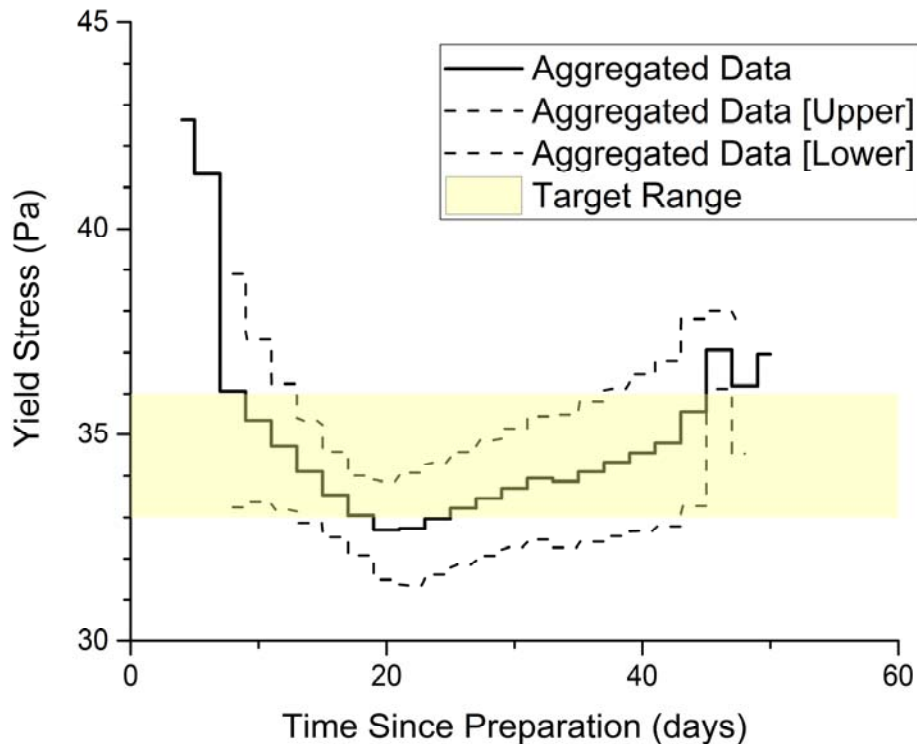


**Figure 3.5.** Aggregated yield stress for the “best” recipe over time. Since the aggregation is based on discrete data, the aggregated data (solid line) represents a mean value in 2-day increments, with lower and upper bounds (dotted lines) representing a standard deviation of the mean.

The aggregate yield stress data of the “best” recipe, after an initial drift downward as the simulant hydrates, is within the target range after approximately 20 days and remains there for most of the rest of the period. There is a small upward shift in the data near the end at elapsed times > 40 days that brings the aggregate data outside of the target range. The aggregate consistency data is within the target range for nearly the entire time period the samples were observed, with a gradual upward drift with time. Near the end of the elapsed time period, the consistency is trending to exceed the target range at elapsed times of approximately > 50 days.

There is some caution to be exercised with the aggregated information to avoid inferring too much regarding the rheology of the “best” recipe at very long times. Though both the yield stress and the consistency appear to have a slight upward trend with time, this would not be expected to continue in perpetuity. It is possible that the measurements were already affected by sample volume limitations during the analysis presented here. Each time the rheology data is collected, the sample is interacted with. Some material is lost during the analysis, and some of the sample was irrecoverably used in measurements of density and weight percent solids. As the sample volume decreases, the ability to accurately represent the original sample also decreases. Thus, given a simulant with enough volume, the upward trend observed in the yield stress and consistency should be less pronounced or negligible.

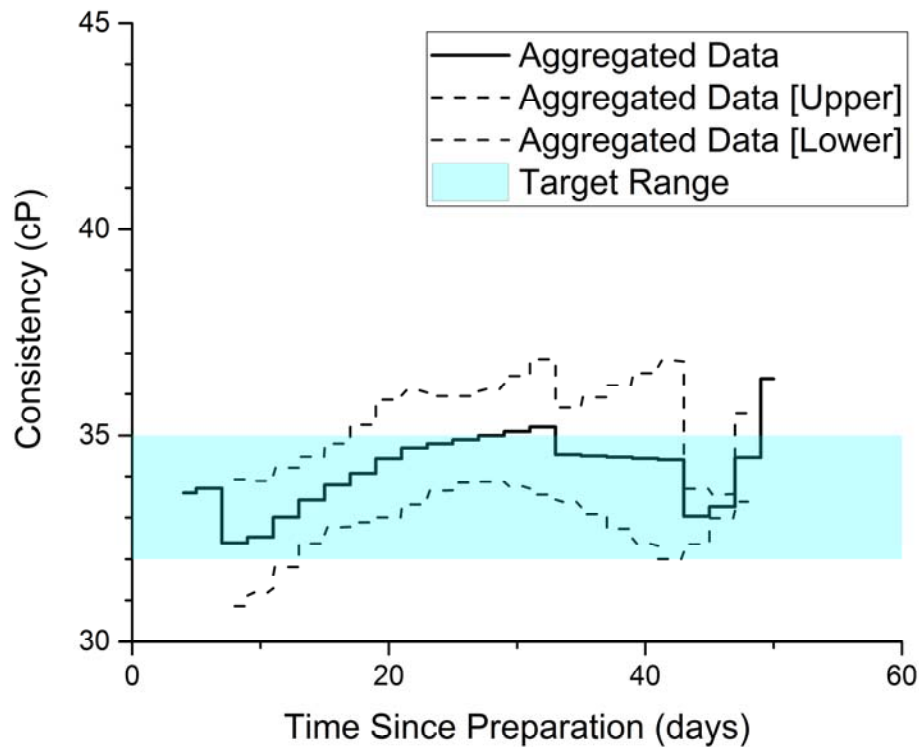


**Figure 3.6.** Aggregated consistency for the “best” recipe over time. Since the aggregation is based on discrete data, the aggregated data (solid line) represents a mean value in 2-day increments, with lower and upper bounds (dotted lines) representing a standard deviation of the mean.

However, it is important to note that the lower and upper bounds generated from the aggregate data are based on only one standard deviation, and thus may underrepresent the actual uncertainty in the samples. If the samples are distributed about the mean in a Gaussian fashion, only ~68% of sample measurements

would be expected within that range. This is concerning when considering the aggregated yield stress, which has mean data in the target range but has lower and/or upper bounds extending outside the range for the majority of the time period. The aggregate yield stress lower bound remaining below 33 Pa until almost 40 days is a particular problem since adjusting from a yield stress that is too low (adding NaCl or clay solids) is more difficult than adjusting from a yield stress that is too high (adding water). It is not clear from the data presented in Figure 3.5 and Figure 3.6 if the magnitude of the uncertainty bounds is due to only having five samples (it is also a discrete, sparse data set) in the aggregate data, or if the uncertainty bounds are representative of the true variation in Bingham parameters with time.

The aggregate data suggests that an aging period of a minimum of 20 days is needed, and a 30-day aging period would be preferred. Monitoring the simulant frequently with time is also recommended to establish the trends of Bingham parameters with time and provide confidence that the simulant materials have the required rheology. As mentioned previously, sample volume limitations affected assessment of the observed upward trend, which may or may not be significant in the same simulant mixture at larger volumes. Given the fairly significant spread in the lower and upper bounds for the Bingham parameters, creating an initial slurry that can be diluted down, i.e., withhold a small fraction of water, once the aged rheology has been measured may be preferable to avoid a rheology that is below the target values.

### 3.4 Rheology of the Recommended Simulant

The rheology of the recommended simulant (and earlier iterations of similar simulant recipes) has been evaluated solely in terms of the yield stress ( $\tau_0^B$ ) and consistency ( $k_B$ ) of the Bingham plastic constitutive equation (see Eq. (2.4)). While the Bingham plastic equation provides a suitable means of modeling the shear rate dependence of stress for the MADC-4 simulant, the Bingham plastic parameters reported in previous pages do not provide detailed information on how the MADC-4 simulant stress response evolves as a function of time (or consecutive rheology measurements) and do not capture information about flow curve and sample hysteresis that may be of interest to aging, preparing, and measuring the slurry. Likewise, reporting only the best-fit parameters does not provide direct evidence of Bingham plastic model suitability. To address these deficiencies, an example flow curve measurement for the recommended MADC-4 simulant recipe (sample NN-028) is provided in Figure 3.7 and is discussed in the rest of this section. Additional flow curve measurements for the recommended simulant measured over a period of approximately 2 to 33 days following preparation are presented in Appendix A. It should be noted that while the exact yield stress and consistency values derived from these measurements may be different, the overall stress response of the fluid is relatively consistent and is well represented by the example given in Figure 3.7.

Figure 3.7A shows three consecutive flow curve measurements on MADC-4 sample NN-028 after 21 days of aging. As described in Section 2.0 of this document, each flow curve consists of a 5-min shear rate ramp from 0 to 1000 s<sup>-1</sup>, a 1-min shear rate hold at 1000 s<sup>-1</sup>, and a 5-min shear rate ramp from 1000 to 0 s<sup>-1</sup>. The low shear rate behavior is indicative of a yield stress material. However, the true yield behavior is somewhat obscured by operation of the rheometer in a controlled rate (rather than a controlled stress) mode. Overall, the shear rate dependence of the fluid is consistent with a Bingham plastic, Casson, or Herschel-Bulkley model.

Once the material is yielded, the stress increases are essentially linear with increasing shear rate. Close examination of the shear stress versus shear rate curves finds a slight downward curvature in most measurements that is consistent with the “shear-thinning” behavior described in Figure 2.3; however, the behavior is not universal. A notable deviation is the step increase in slope that occurs during the first shear rate ramp at  $600 \text{ s}^{-1}$ . This increase is characteristic of the recommended simulant and appears to occur during the first up-ramp of many (if not all) flow curve measurements (see Appendix A). It is believed that this step increase is indicative of typical shear thickening behavior associated with dense colloid suspensions and attributed to hydrodynamic clustering or particle contact forces [cf; Lin et al. (2015) and Bian et al. (2014)]. This assertion is consistent with the steady time and/or shear history dependent increase in the stress response of the sample over runs 1, 2, and 3.<sup>1</sup> For the second and third up-ramps, no further step increases in slope occur at  $600 \text{ s}^{-1}$ , suggesting that shear-thickening is gradual or occurs only at the highest shear rates. That is, once the initial thickening is complete, both up-ramp and down-ramp are nearly linear. Evidence of the slight downward curvature is still apparent in the slight offset that exists between the actual yield stress (inferred by examination of the flow curve data at low shear) and that fit by extrapolation of the Bingham plastic curve (which is fit over  $250$  to  $800 \text{ s}^{-1}$ ). Given the shear-thickening behavior observed at shear rates above  $600 \text{ s}^{-1}$ , it is possible that the downward curvature (i.e., shear thinning) is due in part to relaxation of the clay below shear rates needed to sustain the hydrodynamic or contact forces giving rise to the shear-thickening behavior observed in the run 1 of the flow measurements.

As indicated above, fits of the flow curve data using the Bingham plastic model are shown in Figure 3.7B-D for runs 1-3, respectively. The solid portion of the best-fit line denotes the fitting region, whereas the dashed portion of the best-fit line corresponds to the shear rate range to which the fit is extrapolated. The best-fit yield stress and consistency are reported in the upper left-hand corner of the sub-figures. The overall quality of the fit is good with coefficient of determinations ( $R^2$  values) of 0.997 for most fits. The Bingham model provides a reasonable representation of the flow curve behavior. Because of the slight downward curvature in the flow curves, the Bingham fit overestimates the actual yield stress of the slurry by approximately 1 Pa. The gradual increase in the Bingham parameters in runs 1, 2, and 3 is a result of the shear thickening behavior identified above. Although both yield stress and consistency increase, the yield stress increase ( $\sim 15\%$ ) is larger than the corresponding increase in consistency ( $\sim 2\%$ ).

As demonstrated by the discussion above, the rheological behavior of the recommended MADC-4 formulation is complex and exhibits path (history) dependent rheology (i.e., flow curve hysteresis). Similar complexity was not identified in previous physical simulant development efforts using a mixture of kaolin and bentonite clay. However, earlier efforts typically targeted yield stresses of 30 Pa that were slightly lower than the 34.5 Pa yield stress targeted. It is possible that the increase in clay solids loading needed to achieve this 15% increase in yield stress over previous efforts shifts the clay solids loading into a regime where the hydrodynamic and contact forces that cause shear thickening to occur in the shear rate range typically evaluated in PNNL’s simulant development efforts ( $0$  to  $1000 \text{ s}^{-1}$ ). While the resultant slurry rheology is essentially that of a Bingham plastic after shear, there remains some underlying shear-thicken and shear-thinning behavior that confounds an exact and consistent determination of the

---

<sup>1</sup> It should be noted that increase in the stress response during repeated measurements on the same sample could also indicate evaporation of water from the sample, which would increase the clay concentration and, as a result, the measured rheology. Some evaporation is likely, as the total measuring time of the sample is on the order of 45 minutes. Sample evaporation would not explain the step increase in slope at  $600 \text{ s}^{-1}$ .

recommended simulant rheology. For example, the onset of shear thickening at  $600\text{ s}^{-1}$  requires that corresponding rheology measurements at the SHSVD test stand use the same flow curve measuring routine to replicate the rheological determinations shown in Figure 3.7 and in Appendix A.

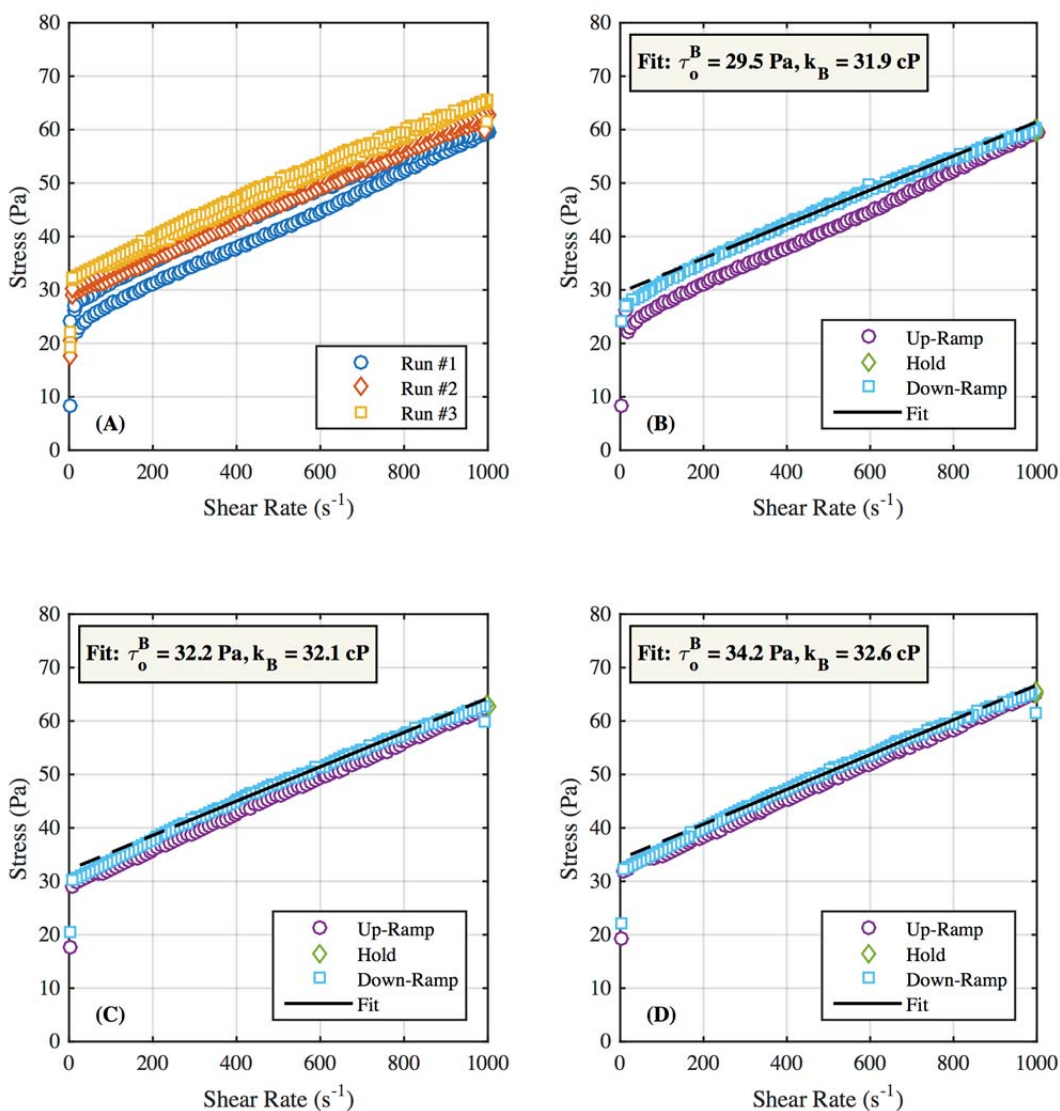


**Figure 3.7.** Flow curves for NN-028 after 21 days of aging showing all three consecutive flow curves on the same plot (A) and individually (B – first, C – second, and D – third). Individual flow curves show the best-fit Bingham plastic for a shear rate range of  $250\text{ to }800\text{ s}^{-1}$  (solid black line) and extrapolated to the full range of shear rates measured (dashed line).

### 3.5 Simulant Technical Concerns and Recommendations

During the course of obtaining the “best” recipe described in the previous section, a number of technical concerns arose from the data collected to date. These concerns, in no particular order, are as follows:

- The “best” recipe recommends a higher nominal amount<sup>1</sup> of clay solids (35.7 wt%) to achieve the target Bingham parameters than historical non-Newtonian slurry data or recent past work. Bontha et al. (2007) report achieving a rheology of approximately 30 Pa/30 cP using a 80:20 kaolin/bentonite slurry at nominally 27 wt%. More recently, Daniel et al. (2013) and Schonewill et al. (2013) describe using a 80:20 kaolin/bentonite clay slurry of approximately 32 to 32.5 wt% to achieve a rheology of 30 Pa/30 cP. Other recent testing used a clay solids loading of around 33.4 wt% (Schonewill et al. [2015]) to achieve an average consistency of ~34 cP. Overall, past work has generally achieved Bingham parameters using 80:20 kaolin/bentonite slurries with less clay solids than recommended in this document. Note also that all of these previous experimental studies mixed the clay slurries at much larger scale, i.e., from fifty to thousands of gallons. Some variation in clay material is expected (moisture content, particle size and structure) and may be producing some of the difference in this case. Another possible contributor is variation in the water source (RCW) used in this study.
- The rheograms, with the exception of the measurements performed on samples that did not contain NaCl, had varying degrees of hysteresis (refer to Appendix A). The hysteresis was found to decrease slightly with time after the initial rheology measurements, i.e., the impact is reduced with simulant age. The hysteresis was unexpected and increases the variability in the data collected from rheology measurements. In past (unpublished) work, adding NaCl to hydrated clay slurries did not lead to increased hysteresis. It is possible that there are some complex particle-particle interactions occurring in these systems (clay solids, LDSP, and salt) or solution chemistry effects that are not well understood.
- The uncertainty range established at the onset of this work for the rheological properties of the recommended simulant is very precise ( $\pm 1.5$  Pa or cP). There is sample-to-sample variability (in samples with the same formulation or recipe measured at similar times) that approaches or exceeds this uncertainty range. Some of the observed variability may be due to the previously described hysteresis, and to reiterate, this may be related to particle-particle or particle-fluid interactions that are occurring in the simulant.
- Samples with the same formulation or recipe displayed different aging behavior. Assuming the samples eventually “settle” down into the target range, this may not be problematic. However, it could also be indicative of a sensitivity to mixing or other solution conditions (pH, or variations in dissolved species in RCW, for example). Differences in conductivity and pH of various slurries were observed during preparation, and these generally resulted in different rheological behavior. These differences could arise from changes in the ions in the source water or local variations in mixing that have brought components together in concentrations that differ from the bulk concentration. Given that the rheological properties of bentonite are sensitive to small changes in pH (Choo and Bai [2015]), variation in pH is a potential reason for the inconsistent batch-to-batch simulant rheology observed herein. Since the larger scale simulant is expected to be prepared with RCW at a specific

---

<sup>1</sup> Recall that the nominal amount in this case indicates the weight percent of clay solids “as-is” and does not account for variations in the moisture content of the clay, i.e., it is not a dry basis.

time, pH variation impacting simulant preparation is likely a minor concern. However, the RCW used to make up the larger scale simulant, if it has a significantly different pH than the RCW used in this study, may yield different transient behavior of measured Bingham parameters.

- The rheological behavior of the “best” recipe is unknown when it is scaled up to volumes greater than 1 L. One possible explanation for the variability in rheology between samples with the same formulation is variations in mixing. If this was the case, the problem may manifest differently at larger scale due to the use of industrial mixing equipment, exposure to high shear rate pumps, and inter-tank transfers.

With this list of concerns in mind, some recommendations can be offered to hedge against the uncertainties inherent in preparing the “best” recipe at larger scale. The intent of the SHSVD test program is to mix the simulant in various sub-batches before combining them together in the test vessel. Each sub-batch will not contain the LDSP, as they will be added directly to the test vessel. Given that, the following recommendations are made:

- Prepare trial batches of the recommended recipe at some reasonably large scale (> 1 L) using the clay materials acquired for use in the SHSVD test program, and monitor their rheological behavior over time for a minimum of 20 days. Monitoring after 20 days can be performed if the rheological behavior still appears to be changing with time.
- Dissolve the NaCl in RCW prior to adding any of the clay solids, following PNNL’s practice at the laboratory scale.
- Allow the simulant sub-batches to hydrate for at least 20 days prior to use in the test vessel. The test schedule can be designed to provide a sufficient time window (best defined based on the behavior of the trial batches mentioned previously) to permit the simulant to age and then adjust the batches (if needed).
- Withhold a small fraction of the water, say 0.3 to 0.5 wt%, from the initial sub-batches to guard against a rheology that is below the target range. The Bingham parameters of these batches, if above the targets, can then be adjusted with the addition of water. Adjustments using water are much more straightforward than adjustments with solids.
- Measure the rheology of multiple aliquots at the time of sampling to establish confidence in the simulant’s Bingham parameters. This will mitigate the impact of sample-to-sample variability.
- Collect samples for rheology that bound important testing activities, i.e., before and after the activity is conducted. This permits the rheological behavior for those activities to be bounded and reduces the risk that the non-Newtonian simulant is discovered to be outside of the target range after several test activities have been performed.
- Anticipate that the rheology of the simulant may change during testing due to evaporation or other testing activities, and be prepared to perform adjustments.
- Consider increasing the maximum target rheology parameters that are acceptable for testing if maintaining the simulant in the precise  $34.5 \pm 1.5$  Pa /  $33.5 \pm 1.5$  cP Bingham parameter range is challenging.

During the simulant development process, several other samples were prepared to address some of these uncertainties. In general, either insufficient information has been collected from those samples or the data

obtained from these samples did not supply additional clarity to what has been observed regarding the general rheological behavior of these clay slurries (and more specifically, the behavior of the “best” recipe). For completeness, the physical property measurements for these samples are presented in Appendix B along with the measurements for all the samples already discussed.

### **3.6 Dry Basis of Recommended Simulant**

In the preceding sections, the simulant recipes have been discussed using nominal clay solids compositions and excluding the LDSP from the mass percentages. Note from Table 2.1 that the MADC-4 non-Newtonian simulant kaolin and bentonite had specific moisture contents (measured experimentally). Depending on the material lot of clay solids that are used and storage conditions, the moisture content may change. This may have minor impacts on the recommended recipe if a nominal clay solids mass percent was used. It is recommended that the moisture content of the kaolin and bentonite used in future batches be measured to determine the impacts. For convenience, the recommended “best” recipe is also provided on a dry basis in the report summary; refer to Table 5.1.



## 4.0 Other Properties of the Recommended Simulant

The preceding section recommended a non-Newtonian simulant formulation (the “best” recipe) for testing. Planned vessel performance tests will measure the properties of simulant samples, including density, total solids, rheology, and composition, to evaluate simulant mixing and solids de-inventory. In this section, the simulant is discussed in terms of the expected simulant quantification methodologies, namely density, total solids, and rheology testing of diluted samples and sieving of the added LDSP from the clay solids used to impart rheology.

### 4.1 Impact of Dilution

It has been proposed that the efficacy of mixing operations be tracked through changes in physical properties of the process vessel fluid as the diluent mixes with the “concentrate.” Specifically, dilution of the clay-based non-Newtonian simulant with water should produce measurable changes in the physical properties of the simulant that can be used to gauge the uniformity of mixing throughout the tank. Three physical properties are considered to gauge local process vessel dilution: slurry rheology, density, and total solids content. Given the composition of the non-Newtonian simulant, the impact of dilution on the latter two properties, density and total solids content, can be readily predicted through simple engineering-based calculations. The accuracy of dilution evaluations relies on the accuracy to which simulant density and total solids can be measured.

Figure 4.1 compares measurements of non-Newtonian simulant density and total solids to their expected values based on mass make-up. This provides important information about the baseline feasibility of evaluating the impact of dilution through density and/or total solids concentrations. For density, the average difference between measured and calculated values is  $0.003 \text{ g mL}^{-1}$ , although differences as large as  $0.008 \text{ g mL}^{-1}$  are observed in the current measurement set. Likewise, the average difference between measured and estimated total solids concentration is approximately 0.4 wt%, with differences as large as 1.0 wt%. Based on Figure 4.1, density measurements do not appear to be preferentially biased high or low. In contrast, measured total solids concentration always appears to be larger than the expected values. It is currently not known if this bias occurs because of sample drying during storage or if the moisture analyzer drying routine used in the current analysis is appropriate for the clay matrix.

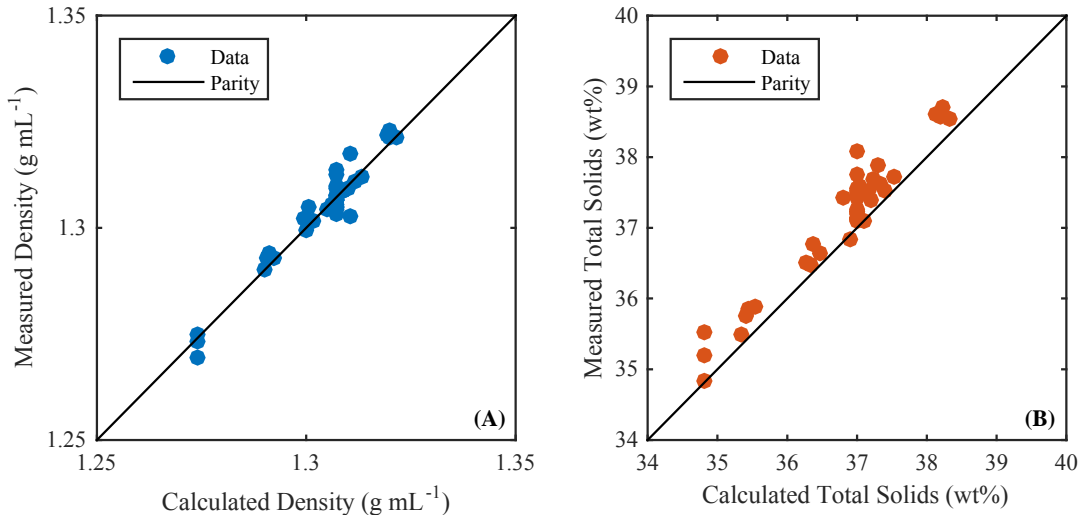


**Figure 4.1.** Parity plots demonstrating the accuracy of non-Newtonian simulant (A) density and (B) total solids concentration measurements. Calculated values are based on the known simulant composition and component densities.

In contrast, no first-principles method exists for estimating the impact of dilution of the rheology of clay-based simulants proposed for use in process mixing tests, and as such, the impact of dilution on non-Newtonian simulant rheology cannot be readily predicted. Thus, the degree of dilution through rheology must be assessed by developing a dilution “calibration curve” for a particular simulant. Development of a detailed calibration curve for diluted rheology is beyond the scope of the current report. However, rheology data for two dilutions of the NN-027 simulant are provided to support a high-level assessment of dilution through rheology.

The dilution ratio  $X$  is defined as

$$X = \frac{V_a}{V_o} \quad (4.1)$$

where  $V_a$  is the volume of the diluent and  $V_o$  is initial volume of slurry “concentrate” in the process vessel before dilution. The dilution ratio  $X$  can be expressed as a volume fraction or percent (with the latter calculated by multiplying the result of Eq. (4.1) by 100%). The density  $\rho$  of the non-Newtonian simulant is given by

$$\rho = \left[ \left( \sum_j \frac{q_j}{\rho_{s,j}} \right) + \frac{1 - \sum_j q_j}{\rho_l} \right]^{-1} \quad (4.2)$$

where  $q_j$  and  $\rho_{s,j}$  are the mass fraction and material density of the  $j^{\text{th}}$  insoluble solid, respectively, in the overall mixture, and  $\rho_l$  is the density of the suspending phase and is a function of the composition of the liquid phase (including dissolved solids) and its temperature. In the current non-Newtonian formulation, there is a single soluble solid (NaCl). At 20°C, the density of NaCl solutions can be approximated by

$$\rho_l = 0.9985 \exp(0.6975 w_{NaCl}) \quad (4.3)$$

where  $w$  is the dissolved solids weight fraction of NaCl in the suspending phase, given by

$$w_{NaCl} = \frac{q_{NaCl}}{q_w + q_{NaCl}} \quad (4.4)$$

where  $q_{NaCl}$  and  $q_w$  are the mass fractions of NaCl and water in the overall simulant mixture, respectively. Finally, the total slurry solids content  $x_{TS}$  is given by

$$x_{TS} = \left( \sum_j q_j \right) + q_{NaCl} \quad (4.5)$$

Given an original non-Newtonian slurry with component mass fractions  $q_i^{(o)}$ , slurry density  $\rho_o$ , total solids  $x_{TS}^{(o)}$ , and initial mass  $m_o$ , the addition of a mass of water  $m_a$  will yield the following dilution ratio:

$$X = \left( \frac{\rho_o}{\rho_w} \right) q_a = s_o q_a \quad (4.6)$$

with  $q_a = m_a/m_o$ . Here,  $s_o$  is the specific gravity of the original slurry concentrate and allows a slightly more compact dilution ratio notation. Dilution with water will shift the mass fraction of insoluble solids, sodium chloride, and total water to

$$q_j^{(f)} = \frac{q_j^{(o)}}{1 + q_a} \quad (4.7)$$

$$q_{NaCl}^{(f)} = \frac{q_{NaCl}^{(o)}}{1 + q_a} \quad (4.8)$$

$$q_w^{(f)} = \frac{q_w^{(o)} + q_a}{1 + q_a} \quad (4.9)$$

where the superscript ( $f$ ) denotes diluted mixture properties. The final mixture density is

$$\rho_f = \left[ \left( \sum_j \frac{q_j^{(f)}}{\rho_{s,j}} \right) + \frac{1 - \sum_j q_j^{(f)}}{\rho_l^{(f)}} \right]^{-1} \quad (4.10)$$

where the final suspending phase density  $\rho_l^{(f)}$  is evaluated at a final dissolved NaCl concentration  $w_{NaCl}^{(f)}$  of

$$w_{NaCl}^{(f)} = \frac{q_{NaCl}^{(f)}}{q_{NaCl}^{(f)} + q_w^{(f)}} \quad (4.11)$$

The final density and dissolved salt concentration are expressed in terms of the final mass fractions because these expressions cannot be easily reduced into terms of original properties. The final total solids concentration is given by

$$x_{TS}^{(f)} = \frac{x_{TS}^{(o)}}{1 + q_a} \quad (4.12)$$

where  $x_{TS}^{(o)}$  is that of the undiluted slurry. The final volume  $V_f$  of the diluted slurry is then

$$V_f = (1 + q_a) \left( \frac{\rho_o}{\rho_f} \right) V_o \quad (4.13)$$

When applied to the non-Newtonian recipe recommended for full-scale testing (see Table 4.1 for simulant properties), these equations allow prediction of the diluted slurry properties as a function of dilution level. However, the intended use of the correlations is to use measured slurry properties to estimate the sample dilution and therefore the local degree of mixing. To this end, a dilution calculation for the recommended non-Newtonian simulant recipe has been performed for dilution ratios ( $X$ ) of 0% to 25%; however, the results of this analysis are presented as the dilution ratio as a function of diluted slurry density (Figure 4.2A) and diluted slurry total solids (Figure 4.2B) to allow conversion of measured slurry properties to local dilution.

Although an exact solution for dilution ratio as a function of either density or dissolved solids concentration cannot be reached because of non-ideal dilution of the salt solution, the salt concentration for the proposed MADC-4 simulant is sufficiently low to allow non-ideal mixing to be neglected without loss of accuracy. Thus, the dilution ratio can be determined directly from measured density and total solids concentrations using

$$X = s_o \left[ \left( \frac{s_o - 1}{s_o} \right) \left( \frac{s_f}{s_f - 1} \right) - 1 \right] \quad (4.14)$$

$$X = s_o \left[ \left( \frac{x_{TS}^{(o)}}{x_{TS}^{(f)}} \right) - 1 \right] \quad (4.15)$$

where the final diluted sample density  $\rho_f$  is expressed as a specific gravity:  $s_f = (\rho_f / \rho_w)$ . Caution should be exercised when applying the dilution equations developed above, as they assume that the fractionation of solids in the mixture is constant during dilution. Failure of this assumption in SHSVD testing would lead to divergence in the estimated dilution ratio and that actually realized in testing. It is recommended that dilution ratio estimates made using the methods outlined in this section be further verified using independent means (such as a tracking changes in concentration of a soluble liquid tracer).

**Table 4.1.** Properties assumed for the undiluted “best” simulant recipe (based on sample NN-027c) for the dilution calculations shown in Figure 4.2.

Property	Symbol	Unit	Value
Mass Fraction:			
Kaolin	$q_k^{(o)}$	wt%	27.1
Bentonite	$q_b^{(o)}$	wt%	6.46
Zirox	$q_z^{(o)}$	wt%	3.10
Basalt	$q_b^{(o)}$	wt%	0.249
Sodium Chloride	$q_{\text{NaCl}}^{(o)}$	wt%	0.0874
Water	$q_w^{(o)}$	wt%	63.0
Dissolved NaCl Concentration	$w_{\text{NaCl}}^{(o)}$	wt%	0.139
Slurry Density	$\rho_o$	g mL <sup>-1</sup>	1.0372
Slurry Total Solids Concentration	$x_{TS}^{(o)}$	wt%	37.01

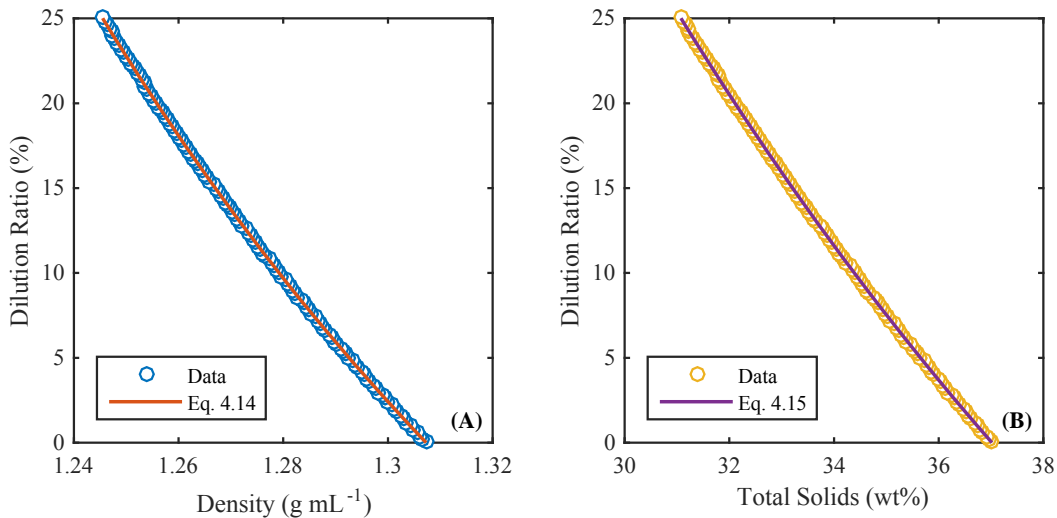


**Figure 4.2.** Calculated sample dilution ratio  $X$  as a function of (A) diluted sample density  $\rho_f$  and (B) diluted sample total solids concentration  $x_{TS}^{(f)}$ . Calculation results are shown for both the exact analysis (open circles) and approximate correlations (Eqs. (4.14) and (4.15) – solid lines).

To assess the validity of the method outlined above for determining local dilution, two bench-scale test dilutions of the NN-027 simulant formulation were performed (denoted as NN-027c, but with the same formulation as NN-027 as described in Section 3.3.1). Specifically, a known mass of water was added to two 50 mL aliquots of simulant to target roughly a 10% and 20% dilution, respectively. The target dilutions simulate expected dilution ratios during the 2000- and 4000-gallon additions of water to the non-Newtonian simulant during non-Newtonian blend test (3B) (see Peurrung and Townson 2016). The density and total solids of these samples were then measured and used to estimate the apparent local dilution using Eqs. (4.14) and (4.15). The results of this assessment are presented in Table 4.2 and Table 4.3.

**Table 4.2.** Measured physical properties of undiluted, 10% diluted, and 20% diluted non-Newtonian simulant (sample NN-027c).

Parameter	Unit	Expected	Measured
Undiluted Slurry			
Pycnometer Density	g mL <sup>-1</sup>	1.3073	1.3073
Graduated Cylinder Density	g mL <sup>-1</sup>	-- --	-- --
Total Solids	wt%	37.01	37.21
10% Diluted Slurry			
Pycnometer Density	g mL <sup>-1</sup>	1.2786	1.2817
Graduated Cylinder Density	g mL <sup>-1</sup>	1.2786	1.278
Total Solids	wt%	34.33	34.87
20% Diluted Slurry			
Pycnometer Density	g mL <sup>-1</sup>	1.2500	1.2530
Graduated Cylinder Density	g mL <sup>-1</sup>	1.2500	1.245
Total Solids	wt%	31.53	31.70

**Table 4.3.** Summary of results for dilution ratio inference by pycnometer density, graduated cylinder density, and total solids concentration for the diluted non-Newtonian simulant (sample NN-027c).

Slurry	Actual Dilution Ratio (%)	Dilution Ratio (%) Inferred By Method		
		Pycnometer Density	Graduated Cylinder Density	Total Solids Concentration
Undiluted	0	-0.01	-- --	-0.70
10% Diluted	10.2	9.03	10	8.04
20% Diluted	22.8	21.3	25	21.9

The previous discussion focuses on the physical properties that should be relatively easy to correlate as a function of dilution. Although it is expected that dilution will lower slurry rheology, the expected change in the Bingham yield stress and consistency of the non-Newtonian simulant cannot be readily predicted. However, a gross measure of dilution can be inferred from rheology simply by comparing the diluted slurry rheology to reference values at defined dilutions. Figure 4.3 presents a limited set of rheology measurements for diluted non-Newtonian simulant to facilitate such comparisons. However, as with the density and total solids formulations, segregation of dense solids may affect the accuracy of such inferences.

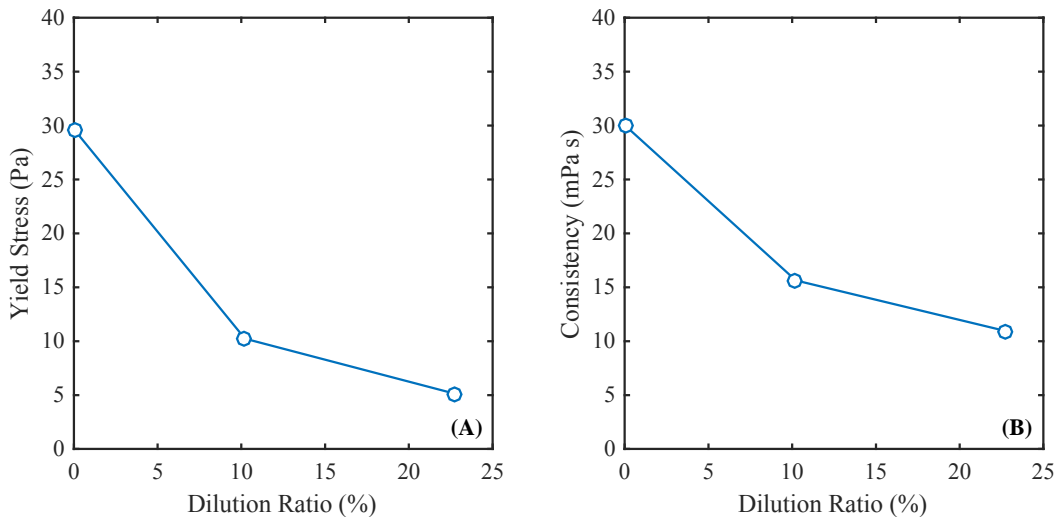


**Figure 4.3.** Measured NN-027c non-Newtonian slurry rheology as a function of dilution ratio: (A) Bingham yield stress and (B) Bingham consistency. Bingham plastic constitutive equation parameters were derived by fitting down-ramp flow curve data over shear rates of 250 to 800  $s^{-1}$ .

## 4.2 Impact of Temperature on Rheology

The impact of temperature on non-Newtonian rheology is difficult to predict from a first-principles basis. Although it is expected that an increase in temperature will reduce the viscosity of the suspending phase, leading to a reduction in the overall apparent viscosity of the slurry, the impact of temperature on the inter-particle interactions yielding solid-like behavior (i.e., yield stress) and shear/time-dependent rheology is unknown. For this reason, the rheology of the proposed MADC-4 non-Newtonian simulant has been measured as a function of temperature both with and without the addition of LDSP (i.e., basalt and Zirox). The results of these measurements are summarized in Figure 4.4. The data point shown at 30 °C for the no LDSP slurry was measured twice and showed the same increase in yield stress for each measurement; it is not clear at present why this value deviates from the downward trend observed for the consistency and the full simulant.

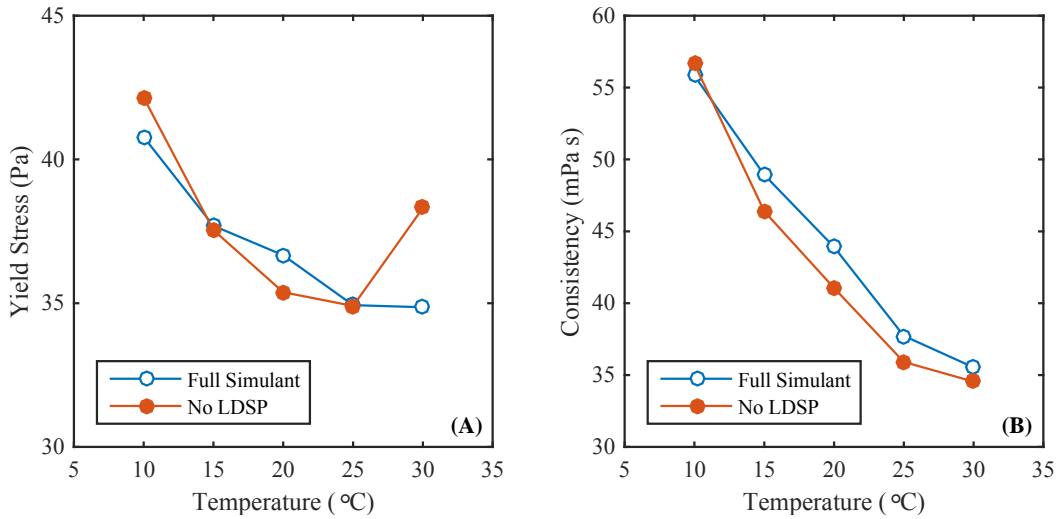


**Figure 4.4.** Non-Newtonian simulant rheology as a function of temperature: (A) Bingham yield stress and (B) Bingham consistency. Bingham plastic constitutive equation parameters were derived by fitting down-ramp flow curve data over shear rates of 250 to 800 s<sup>-1</sup>. Results are shown for the simulant with (sample NN-028) and without (sample NN-029) LDSP.

### 4.3 Simulant Sieving

One liter samples of the recommended MADC-4 non-Newtonian simulant, both with and without added LDSP, were wet-sieved to evaluate the feasibility of recovering and isolating the added LDSP (i.e., basalt and Zirox solids) from the clay solids that impart fluid rheology. Table 4.4 presents the results of the sieving study. The recovery on each sieve cut is compared to the expected amount of basalt and Zirox solids that are expected to be captured on each sieve to infer the sieved solids contribution from the bentonite and kaolin clays. Both sieving results indicate a total clay crossover of 0.8 to 0.9 g L<sup>-1</sup> into the basalt and Zirox sieve cuts. Specifically, there is no contribution from the clay solids on the 300 μm sieve cut used to separate the basalt from the simulant and approximately 0.7 g L<sup>-1</sup> of clay-derived solids on the 106 μm sieve needed to isolate the Zirox solids. Although sieving of the clay matrix without added LDSP suggests higher contamination of the 106 μm cut, it should be noted that the clay was not sieved through the 250 μm (which appears to isolate ~0.1 g L<sup>-1</sup> of clay solids). Pictures of the sieving results are provided in Figure 4.5 for the clay solids only (no LDSP) and Figure 4.6 for the full simulant.

**Table 4.4.** Sieving results for 1 L of non-Newtonian simulant with (sample NN-031b) and without (sample NN-032b) LDSP demonstrating clay crossover of target basalt and Zirox sieve cuts.

Sieve	Expected Mass (g)	Recovered Mass (g)	Inferred Clay Contamination (g)	Notes
Full simulant				
425 $\mu\text{m}$ (#40)	0	0.04	0.04	Should pass all solids
300 $\mu\text{m}$	1.31	1.31	0	Should capture all basalt solids
250 $\mu\text{m}$ (#60)	0	0.11	0.11	Should pass all Zirox solids
106 $\mu\text{m}$ (#140)	16.33	16.98	0.64	Should capture all Zirox solids
<b>Total Contaminant Mass, g</b>			<b>0.80</b>	
Simulant without MADC-4 LDSP				
425 $\mu\text{m}$ (#40)	---	0.02	0.02	---
300 $\mu\text{m}$	---	---	---	Not measured
250 $\mu\text{m}$ (#60)	---	---	---	Not measured
106 $\mu\text{m}$ (#140)	---	0.85	0.85	---
<b>Total Contaminant Mass, g</b>			<b>0.87</b>	

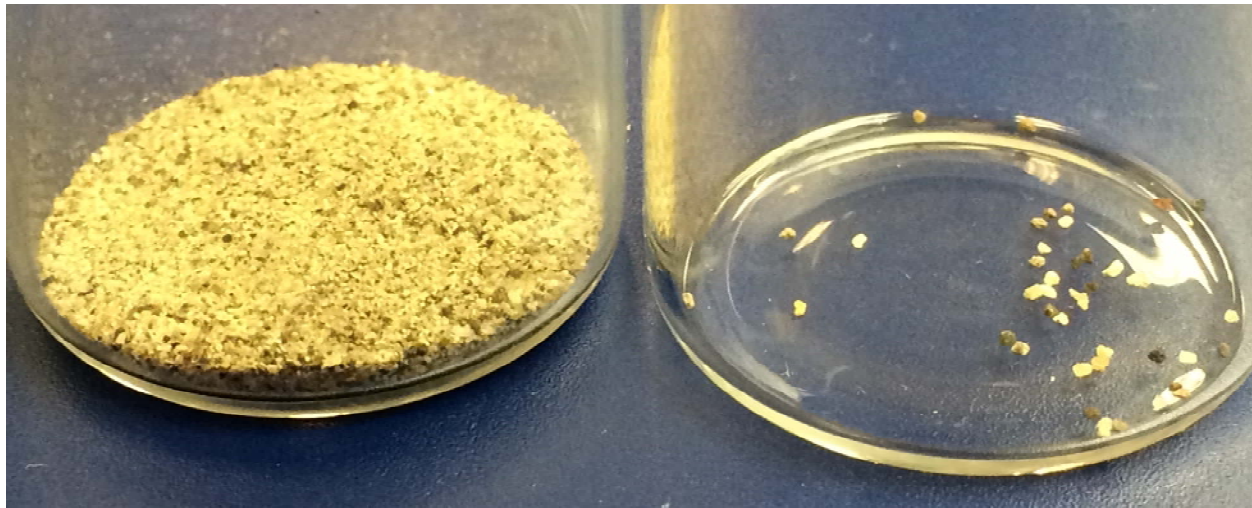


**Figure 4.5.** Images of sieved fractions of the 80:20 bentonite:kaolin clay mixture used in the MADC-4 non-Newtonian simulant. Left: 106  $\mu\text{m}$  sieve cut, Right: 425  $\mu\text{m}$  sieve cut.

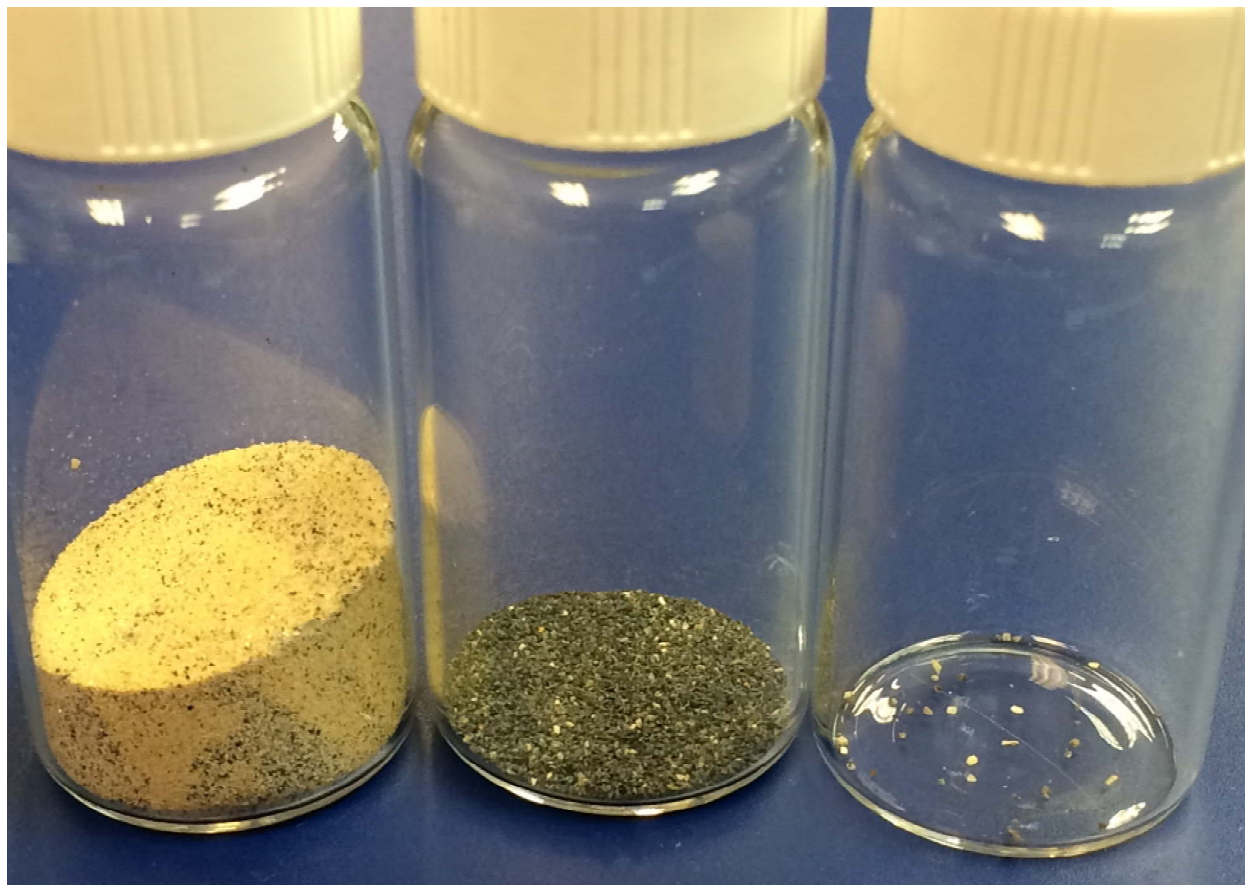


**Figure 4.6.** Images of sieved fractions of the MADC-4 non-Newtonian simulant. From left to right: 106  $\mu\text{m}$  sieve cut (Zirox solids and clay cross-over product; see Figure 4.5), 300  $\mu\text{m}$  sieve cut (basalt solids), and 425  $\mu\text{m}$  sieve cut (large clay particles; see Figure 4.5).

## 5.0 Summary and Conclusions

This document has reported the development and recommended composition and physical properties of the MADC-4 non-Newtonian simulant for testing of the SHSVD vessel for the WTP. The recommended recipe is listed in Table 5.1. The recipe is sensitive to the order of addition, and should be prepared using the following steps:

1. Dissolve the sodium chloride into RCW.
2. Add the bentonite mass in a 1:1 pre-mixed bentonite and kaolin solids mixture (to prevent the bentonite from clumping) to the RCW mixture.
3. Add the remainder of the required kaolin solids to the mixture generated in step 2.
4. Add basalt and Zirox solids.
5. Mix thoroughly for approximately 12 hours.
6. Add biocide to 100 ppm by volume.

This recipe should be approached with some caution, as significant issues arose when optimizing the formulation to meet the strict rheological targets for SHSVD testing. These issues are:

- The recommended recipe differs significantly from clay recipes used to hit the same rheology targets in previous work.
- An unexpected time-dependency is observed in the simulant rheology (characterized by significant flow curve hysteresis); this hysteresis has not been observed in similar clay simulants used in previous testing and increases uncertainty in measured rheology.
- Sample-to-sample and batch-to-batch variability in the simulant rheology is on the order of (if not larger than) the target rheology range, i.e.  $\pm 1.5$  units (Pa or cP).
- The recommended recipe exhibited substantial rheology aging behavior (i.e., how rheology changed with time) that may impact testing timelines.

These factors, combined with the fact that scale-up of the simulant recipe has not been demonstrated, will make it difficult to 1) know if the recipe is aging correctly during large-scale make-up (such that SHSVD test staff have confidence that the recipe will indeed hit the desired rheology targets) and 2) adjust the simulant recipe to meet the desired targets should large-scale aging diverge from that observed during simulant development.

Other findings reported here include the presence of large clay particles within the size range of the added LDSP that originate from the dry clay powders. The basalt and Zirox can be removed/recovered from the clay matrix by sieving; however, for this to be effective the large clay particles will need to be removed from the clay powders, notably the bentonite, prior to simulant make-up.

**Table 5.1.** Summary of recommended recipe (dry-basis) and properties for the MADC-4 non-Newtonian simulant

Composition and Properties	Unit	Value
Composition (Dry Basis)		
Total Water	wt%	62.99
Richland City Water	wt%	62.06
Moisture from Clays	wt%	0.93
Clay	wt%	33.58
Kaolin Clay (Dry)	wt%	27.11
Bentonite Clay (Dry)	wt%	6.46
Zirox	wt%	3.10
Basalt	wt%	0.25
Sodium Chloride	wt%	0.09
Average Properties		
Dissolved NaCl Concentration	wt%	0.14
Slurry Density <sup>(a)</sup>	g mL <sup>-1</sup>	1.311 ± 0.003
Slurry Total Solids Concentration <sup>(a)</sup>	wt%	37.67 ± 0.35
Slurry Yield Stress <sup>(b)</sup>	Pa	34.0 ± 2.2
Slurry Consistency <sup>(b)</sup>	mPa s	34.9 ± 2.1
<p>(a) Average of four samples (NN-022, NN-026, NN-027, and NN-028).  The uncertainty shown is one standard deviation.</p> <p>(b) Average of five samples (NN-022, NN-026, NN-027, NN-028, and NN-029) for measurements taken at greater than 20 days of age.  The uncertainty shown is one standard deviation.</p>		

## 6.0 References

ASME NQA-1-2000. *Quality Assurance Requirements for Nuclear Facility Applications*. American Society of Mechanical Engineers, New York, New York.

Bian, X, S Litvinov, M Ellero, and NJ Wagner. 2014. “Hydrodynamic shear thickening of particulate suspension under confinement.” *Journal of Non-Newtonian Fluid Mechanics*, 213: 39–49.

Bontha JR, DE Kurath, AP Poloski, WC Buchmiller, WH Combs, ED Johnson, HC Webber, and KL Herman. 2007. *Pulse Jet Mixer Controller and Instrumentation Testing*. PNWD-3828; WTP-RPT-146 Rev. 0, Pacific Northwest National Laboratory, Richland, WA.

Choo KY and Bai K. 2015. “Effects of Bentonite Concentration and Solution pH on the Rheological Properties and Long-term Stabilities of Bentonite Suspensions.” *Applied Clay Science*, Volume 108, May 2015, 182–190.

Daniel RC, PA Gauglitz, CA Burns, MS Fountain, RW Shimskey, JM Billing, JR Bontha, DE Kurath, JWJ Jenks, PJ MacFarlan, and LA Mahoney. 2013. *Large-Scale Spray Releases: Additional Aerosol Test Results*. PNNL-22415; WTP-RPT-221, Rev.0, Pacific Northwest National Laboratory, Richland, WA.

DOE/RL-96-68. *Hanford Analytical Services Quality Assurance Requirements Documents*, Volumes 1 and 4. U.S. Department of Energy, Richland Operations Office, Richland, Washington.

Fiskum SK, DT Linn, CA Burns, RA Peterson, NL Canfield, MR Smoot, JA Fort, BE Wells, PA Gauglitz, ST Yokuda, and WL Kuhn. 2017. *Standard High Solids Vessel Design Newtonian Simulant Qualification*. PNNL-26103, RPT-WTP-245, Rev. 0, Pacific Northwest National Laboratory, Richland WA.

Lin, NY C, BM Guy, M Hermes, C Ness, J Sun, WCK Poon, and I Cohen. 2015. “Hydrodynamic and Contact Contributions to Continuous Shear Thickening in Colloidal Suspensions.” *Physical Review Letters*, 115 (22): 228304.

Peterson RA, SK Fiskum, SR Suffield, RA Daniel, PA Gauglitz, BE Wells. 2016. *Simulant Basis for the Standard High Solids Vessel Design*. RPT-WTP-241. Pacific Northwest National Laboratory, Richland, Washington.

Peurrung L and P Townson. 2016. *Test Plan for Mixing Requirements Verification in the Standard High Solids Vessel Design (SHSVD-T) Vessel*. 24590-WTP-ES-ENG-15-033, Rev. 0. Bechtel National Inc., Richland, Washington.

Rassat SD, LM Bagaasen, LA Mahoney, RL Russell, DD Caldwell, and DP Mendoza. 2003. *Physical and Liquid Chemical Simulant Formulations for Transuranic Wastes in Hanford Single-Shell Tanks*. PNNL-14333, Pacific Northwest National Laboratory, Richland, WA.

Schonewill PP, PA Gauglitz, ML Kimura, GN Brown, LA Mahoney, DN Tran, CA Burns, and DE Kurath. 2013. *Small-Scale Spray Releases: Additional Aerosol Test Results*. PNNL-22402; WTP-RPT-222 Rev.0, Pacific Northwest National Laboratory, Richland, WA.

Schonewill PP, EJ Berglin, GK Boeringa, WC Buchmiller, CA Burns, and MJ Minette. 2015. *Scoping Study of Airlift Circulation Technologies for Supplemental Mixing in Pulse Jet Mixed Vessels*. PNNL-24221, Pacific Northwest National Laboratory, Richland, WA.

Slaathaug, E. 2016. *Basis for Simulant Properties for Standard High Solids Vessel Mixing Testing*. 24590-PTF-RPT-PE-16-001, Rev. 0, Bechtel National, Inc., Richland, Washington.

Smith, GL and K Prindiville. 2002. *Guidelines for Performing Chemical, Physical, and Rheological Properties Measurements*. 24590-WTP-GPG-RTD-001, Rev. 0, Bechtel National Inc., Richland, Washington.

Wells BE, DE Kurath, LA Mahoney, Y Onishi, JL Huckaby, SK Cooley, CA Burns, EC Buck, JM Tingey, RC Daniel, and KK Anderson. 2011. *Hanford Waste Physical and Rheological Properties: Data and Gaps*. PNNL-20646, Pacific Northwest National Laboratory, Richland, WA.

## **Appendix A**

### **Rheograms of the Recommended Simulant**



## Appendix A

### Rheograms of the Recommended Simulant

This appendix presents select rheograms for the recommended non-Newtonian (MADC-4) simulant recipe up to approximately 30 days of aging. Each measurement consists of three (or two in limited cases) consecutive flow curve measurements composed of 1) a shear rate “up-ramp” from 0 to 1000 s<sup>-1</sup>, 2) a constant shear rate period at 1000 s<sup>-1</sup>, and 3) a shear rate “down-ramp” from 1000 to 0 s<sup>-1</sup>.

Measurements are reported as shear stress as a function of shear rate, with each figure showing all three flow curves on one plot to demonstrate the impact of repeated shear on the stress response of the sample. In addition, each of the three (or two) consecutive flow curves for each sample are reported individually with the associated best-fit of the down ramp data to the Bingham plastic constitutive equation. Best-fit values for Bingham yield stress ( $\tau_0^B$ ) and Bingham consistency ( $k_B$ ) are reported in the upper left-hand corner of the individual flow curve figures. All fits are limited to a shear rate range of 250 to 800 s<sup>-1</sup>. The best fit result is also shown on the individual figures as a solid black line over the fitted shear rate range and as a dashed line at shear rates outside the fitted region. Rheology data for multiple samples are reported and are ordered in terms of increasing sample age.

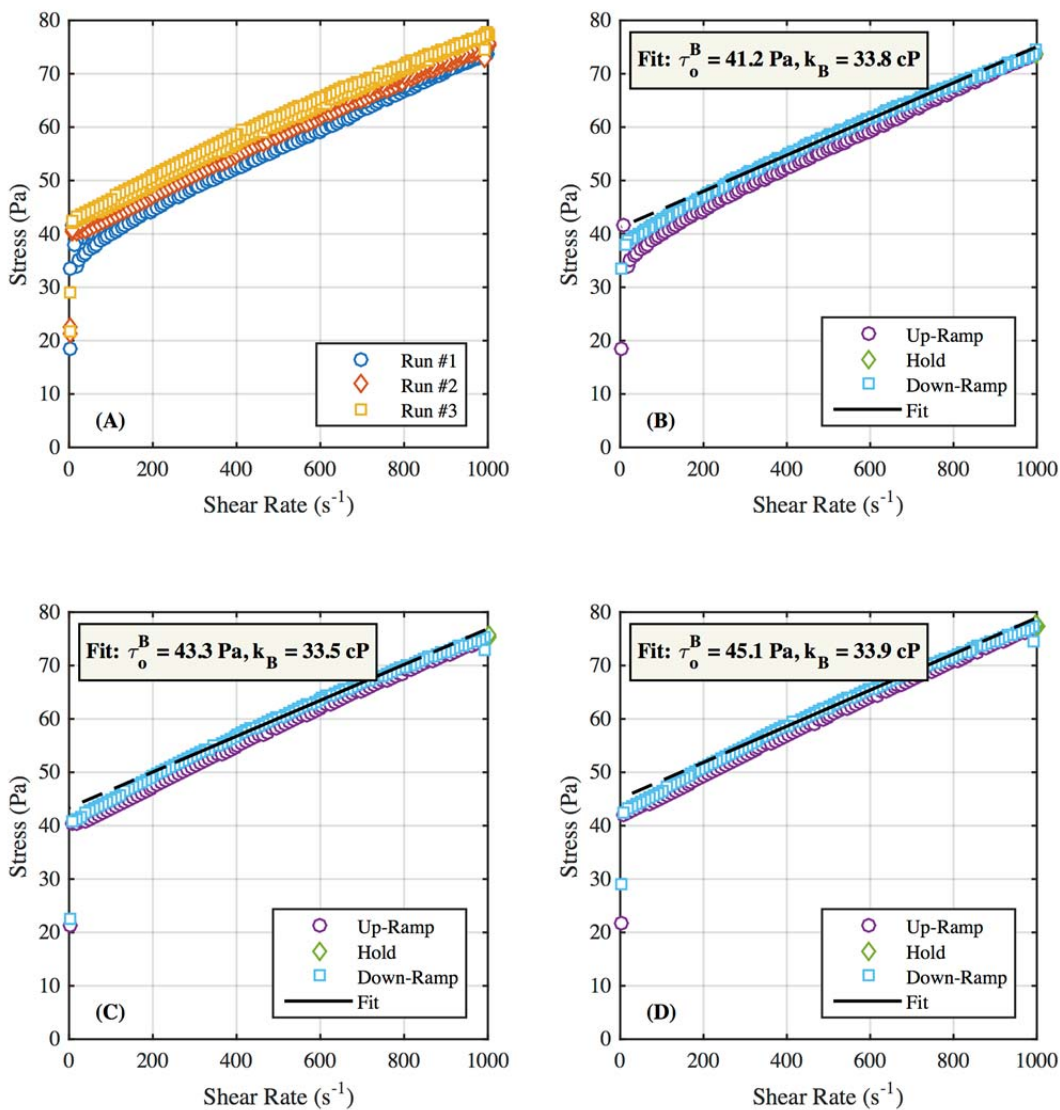


**Figure A.1.** Flow curves for NN-026 after 2.9 days of aging showing all three consecutive flow curves on the same plot (A) and individually (B – first, C – second, and D – third). Individual flow curves show the best-fit Bingham plastic for a shear rate range of 250 to 800 s<sup>-1</sup> (solid black line) and extrapolated to the full range of shear rates measured (dashed line).

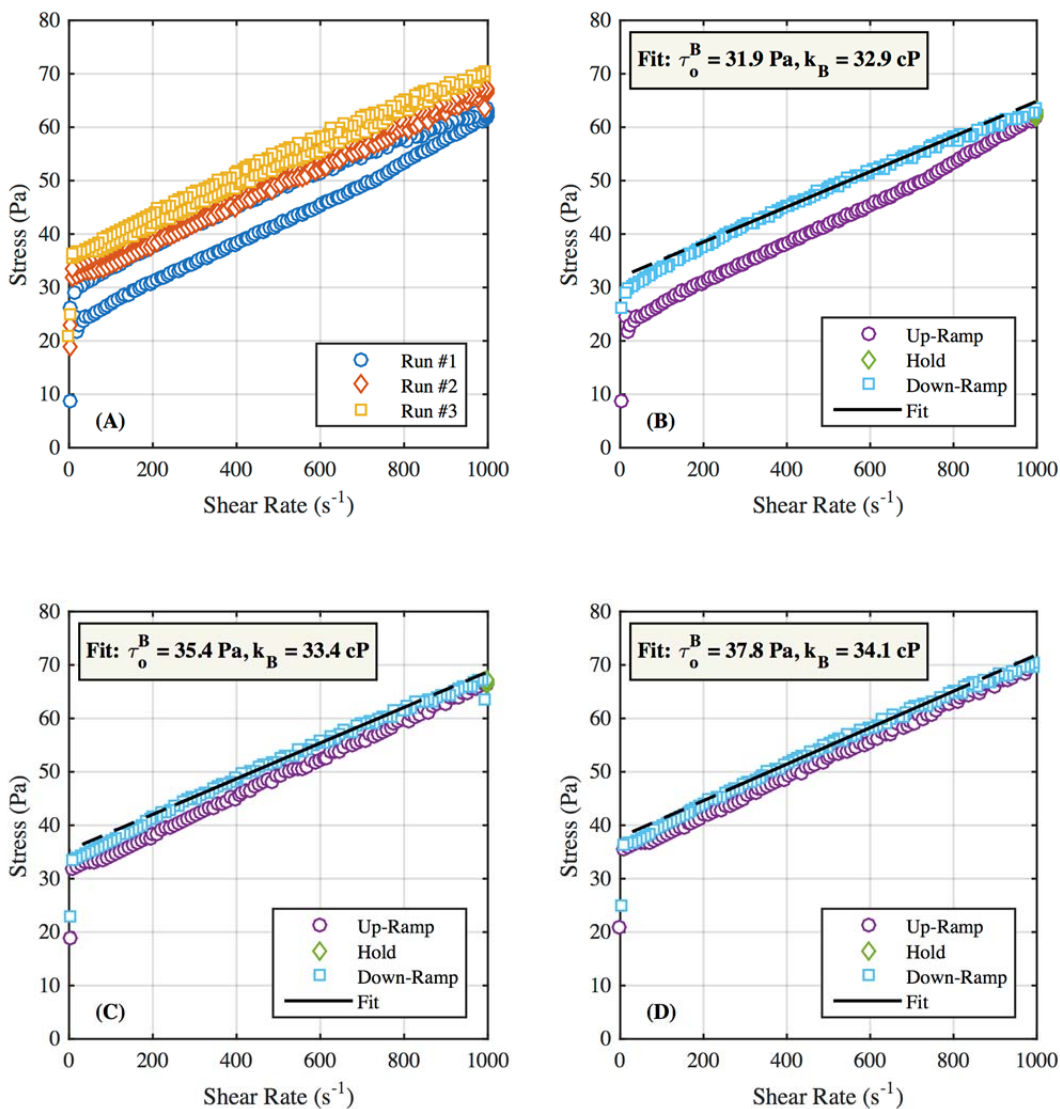


**Figure A.2.** Flow curves for NN-027 after 7.8 days of aging showing all three consecutive flow curves on the same plot (A) and individually (B – first, C – second, and D – third). Individual flow curves show the best-fit Bingham plastic for a shear rate range of 250 to 800 s<sup>-1</sup> (solid black line) and extrapolated to the full range of shear rates measured (dashed line).

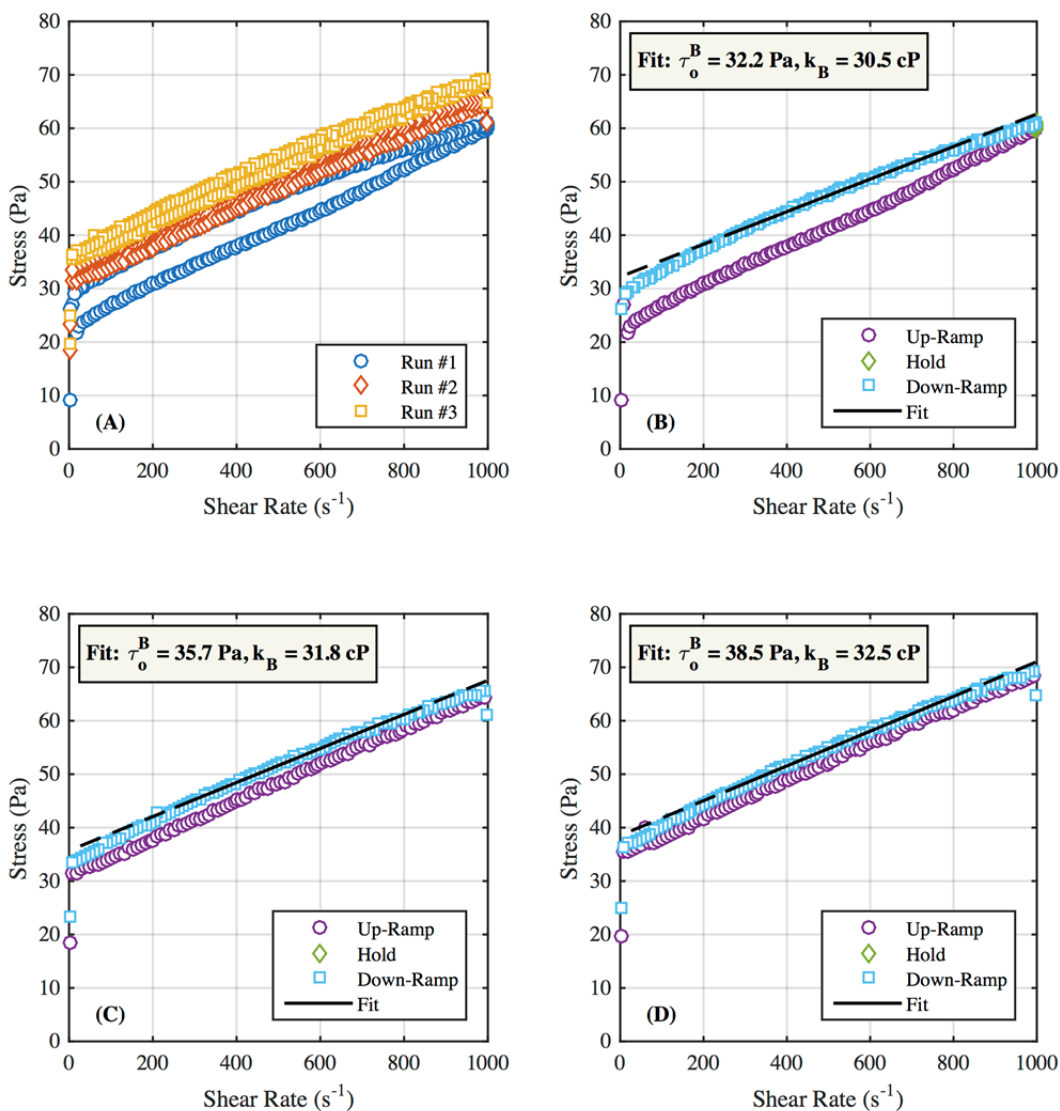


**Figure A.3.** Flow curves for NN-022 after 7.9 days of aging showing all three consecutive flow curves on the same plot (A) and individually (B – first, C – second, and D – third). Individual flow curves show the best-fit Bingham plastic for a shear rate range of 250 to 800  $s^{-1}$  (solid black line) and extrapolated to the full range of shear rates measured (dashed line).

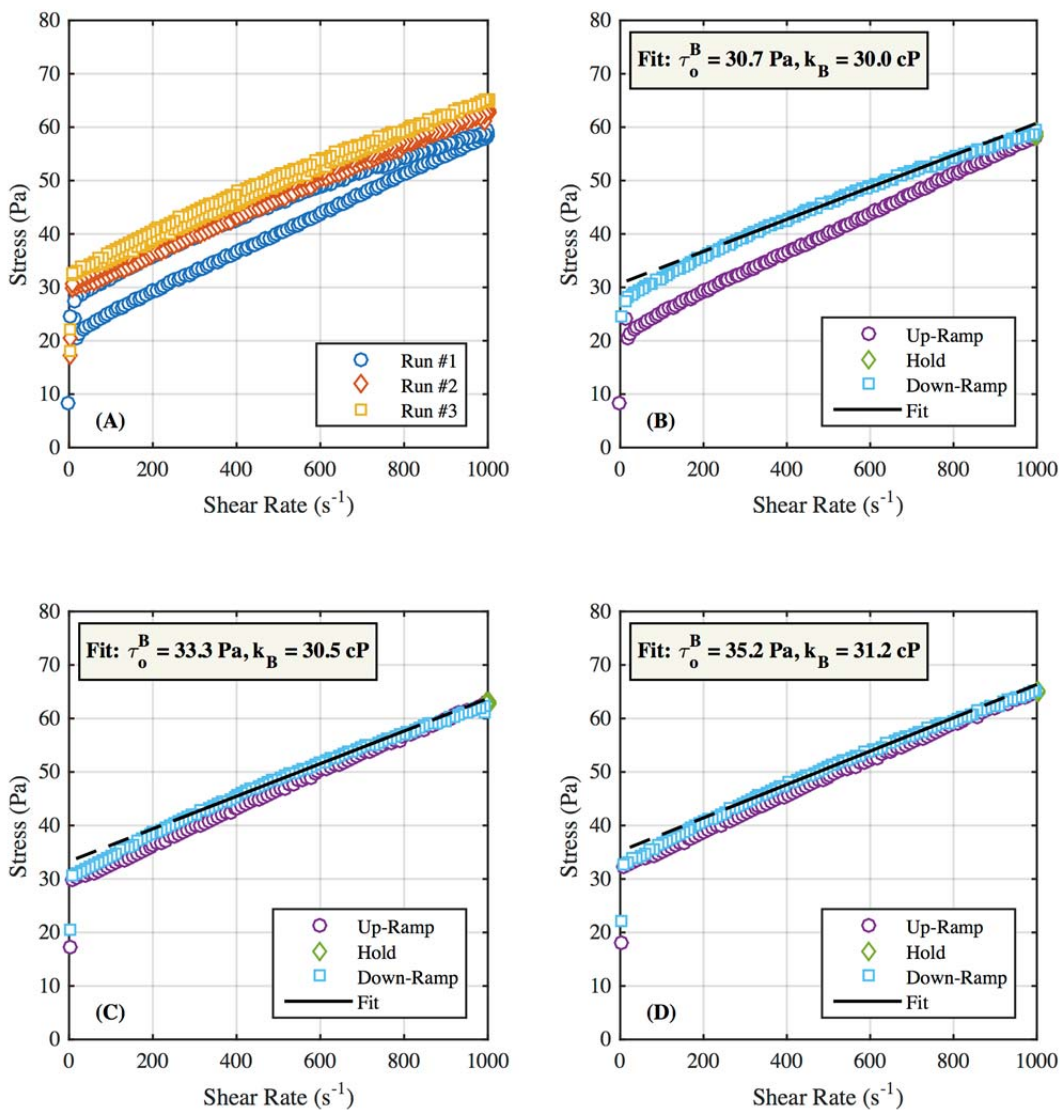


**Figure A.4.** Flow curves for NN-029 after 7.9 days of aging showing all three consecutive flow curves on the same plot (A) and individually (B – first, C – second, and D – third). Individual flow curves show the best-fit Bingham plastic for a shear rate range of 250 to 800  $s^{-1}$  (solid black line) and extrapolated to the full range of shear rates measured (dashed line).

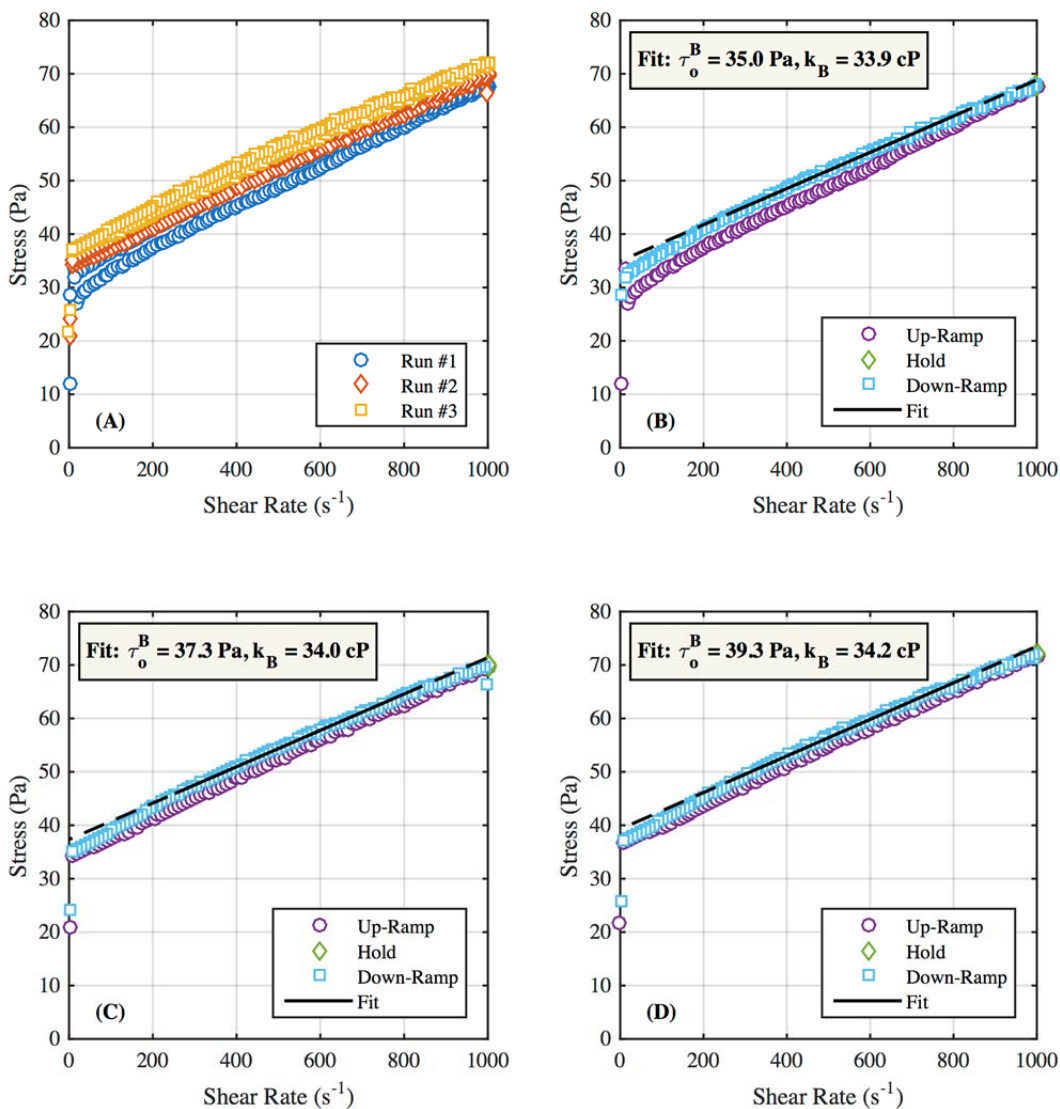


**Figure A.5.** Flow curves for NN-026 after 12 days of aging showing all three consecutive flow curves on the same plot (A) and individually (B – first, C – second, and D – third). Individual flow curves show the best-fit Bingham plastic for a shear rate range of 250 to 800 s<sup>-1</sup> (solid black line) and extrapolated to the full range of shear rates measured (dashed line).

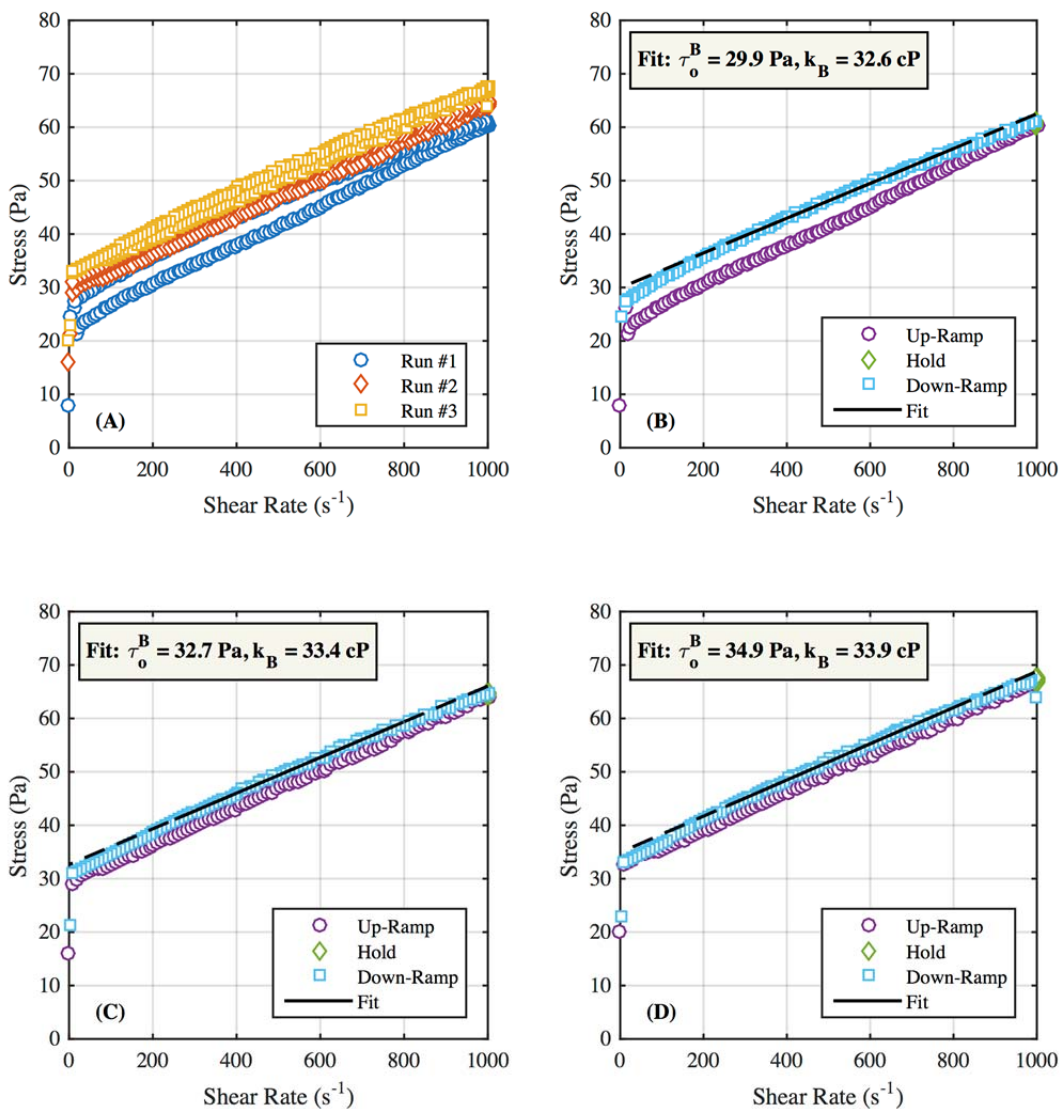


**Figure A.6.** Flow curves for NN-022 after 15 days of aging showing all three consecutive flow curves on the same plot (A) and individually (B – first, C – second, and D – third). Individual flow curves show the best-fit Bingham plastic for a shear rate range of 250 to 800 s<sup>-1</sup> (solid black line) and extrapolated to the full range of shear rates measured (dashed line).

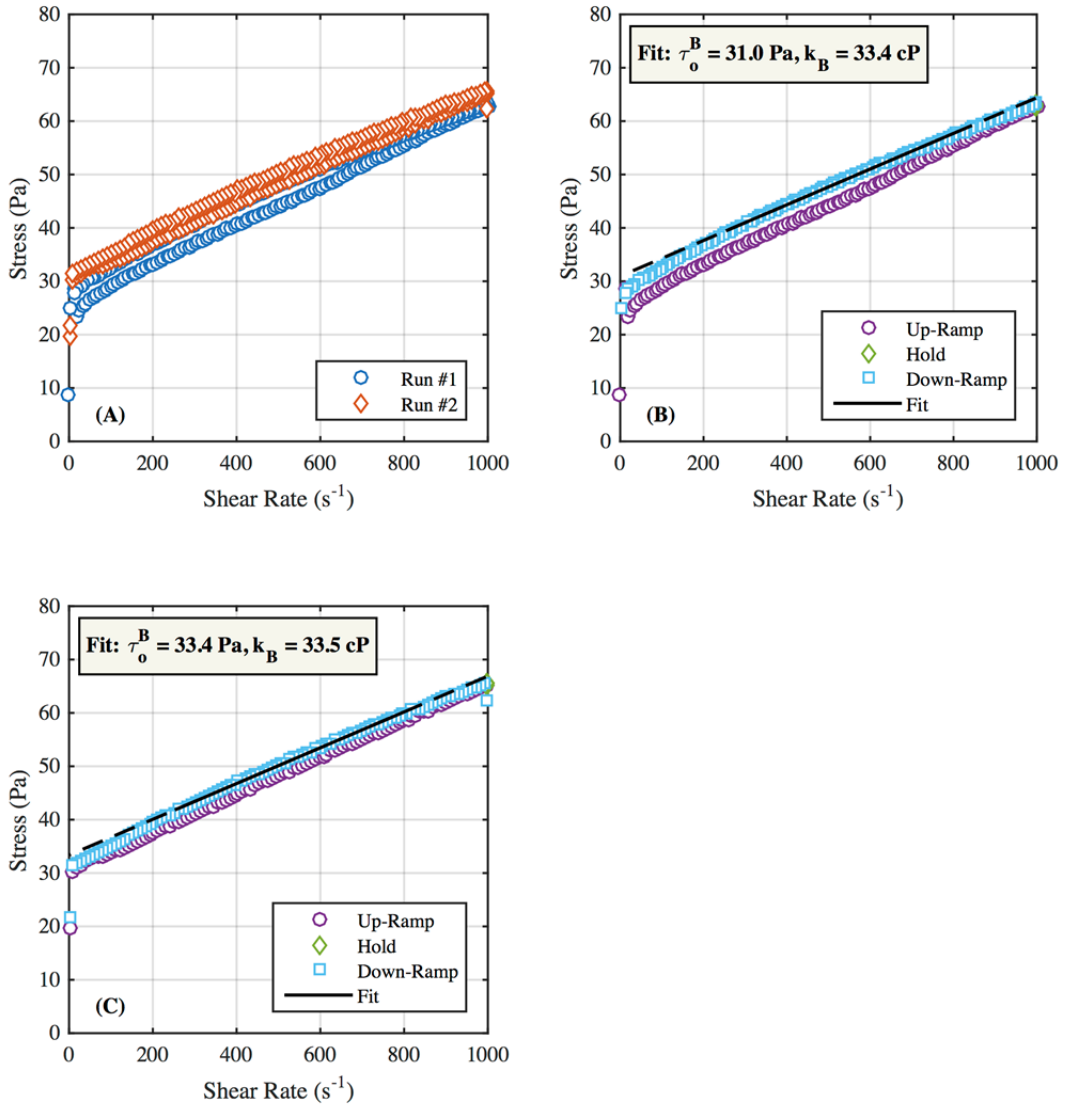


**Figure A.7.** Flow curves for NN-026 after 19 days of aging showing two consecutive flow curves on the same plot (A) and individually (B – first and C – second). Individual flow curves show the best-fit Bingham plastic for a shear rate range of 250 to 800  $s^{-1}$  (solid black line) and extrapolated to the full range of shear rates measured (dashed line).

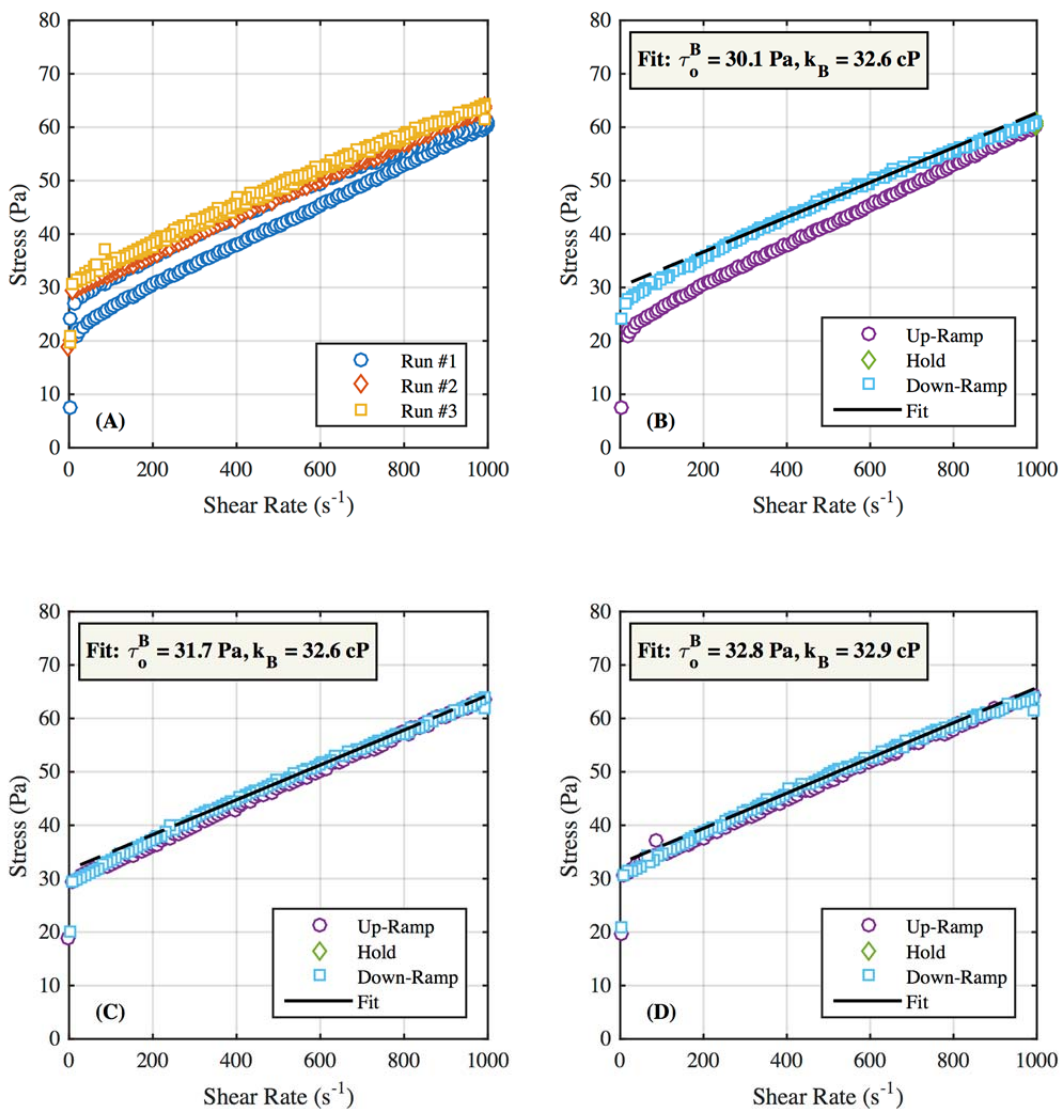


**Figure A.8.** Flow curves for NN-022 after 21 days of aging showing all three consecutive flow curves on the same plot (A) and individually (B – first, C – second, and D – third). Individual flow curves show the best-fit Bingham plastic for a shear rate range of 250 to 800  $s^{-1}$  (solid black line) and extrapolated to the full range of shear rates measured (dashed line).

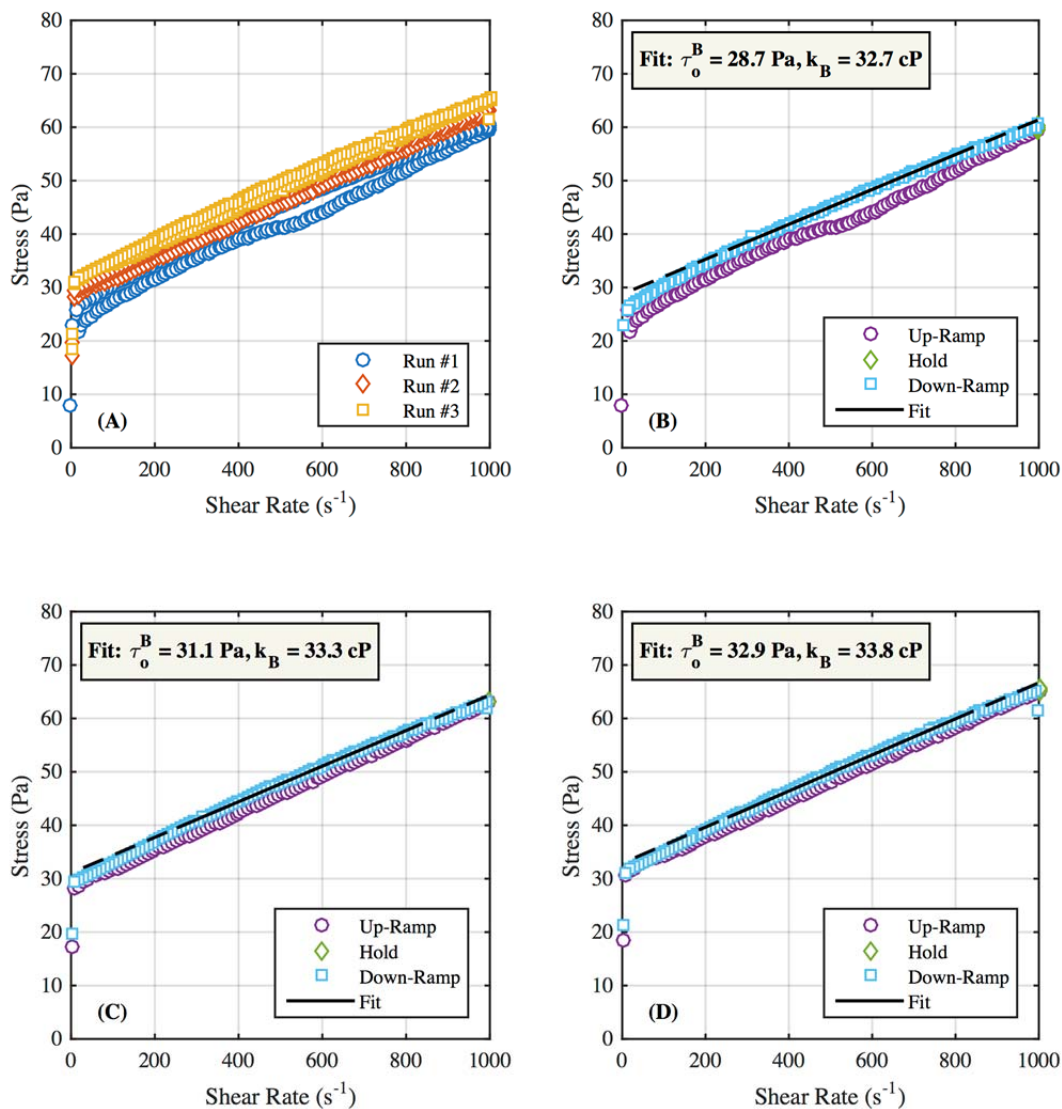


**Figure A.9.** Flow curves for NN-027 after 21 days of aging showing all three consecutive flow curves on the same plot (A) and individually (B – first, C – second, and D – third). Individual flow curves show the best-fit Bingham plastic for a shear rate range of 250 to 800 s<sup>-1</sup> (solid black line) and extrapolated to the full range of shear rates measured (dashed line).

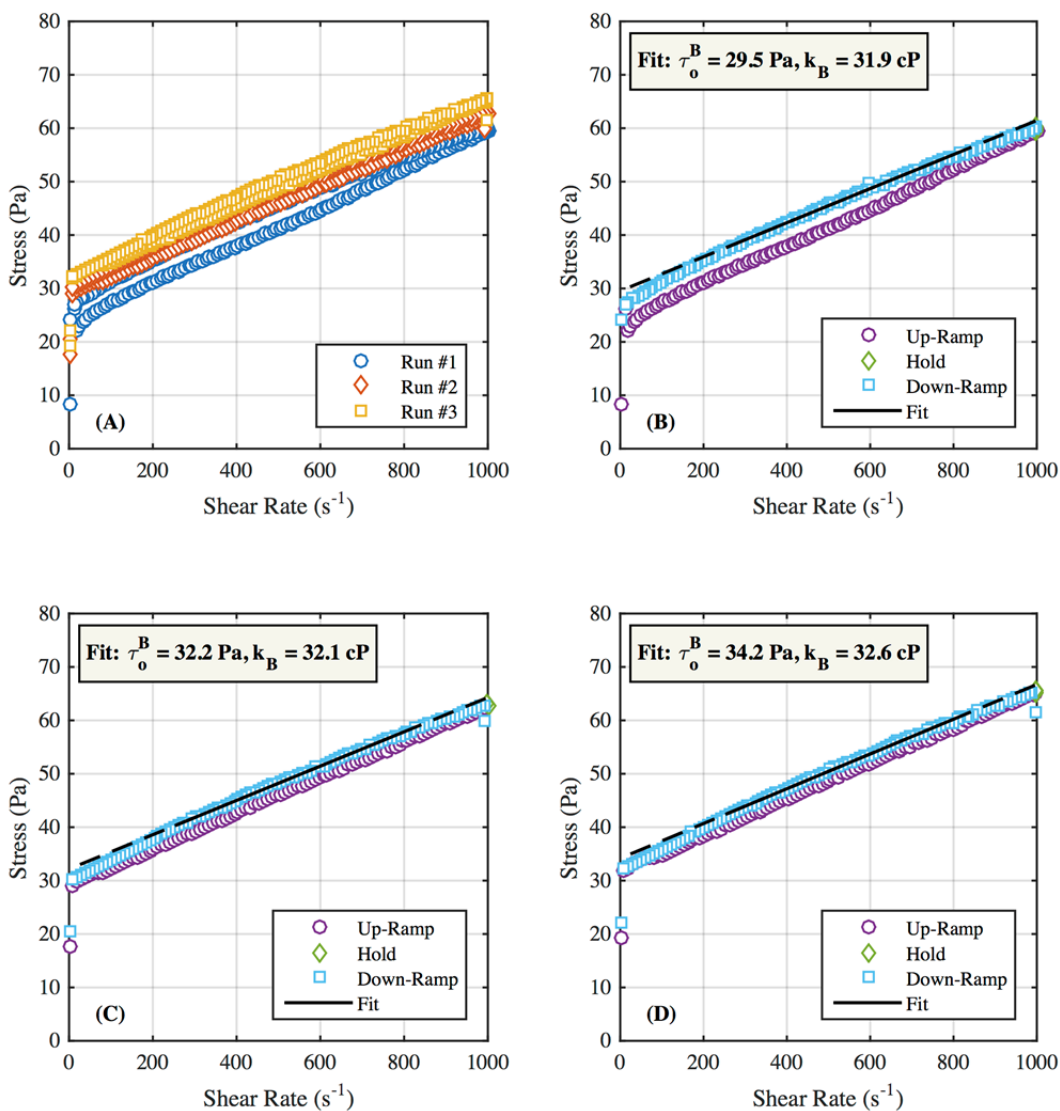


**Figure A.10.** Flow curves for NN-028 after 21 days of aging showing all three consecutive flow curves on the same plot (A) and individually (B – first, C – second, and D – third). Individual flow curves show the best-fit Bingham plastic for a shear rate range of 250 to 800 s<sup>-1</sup> (solid black line) and extrapolated to the full range of shear rates measured (dashed line).

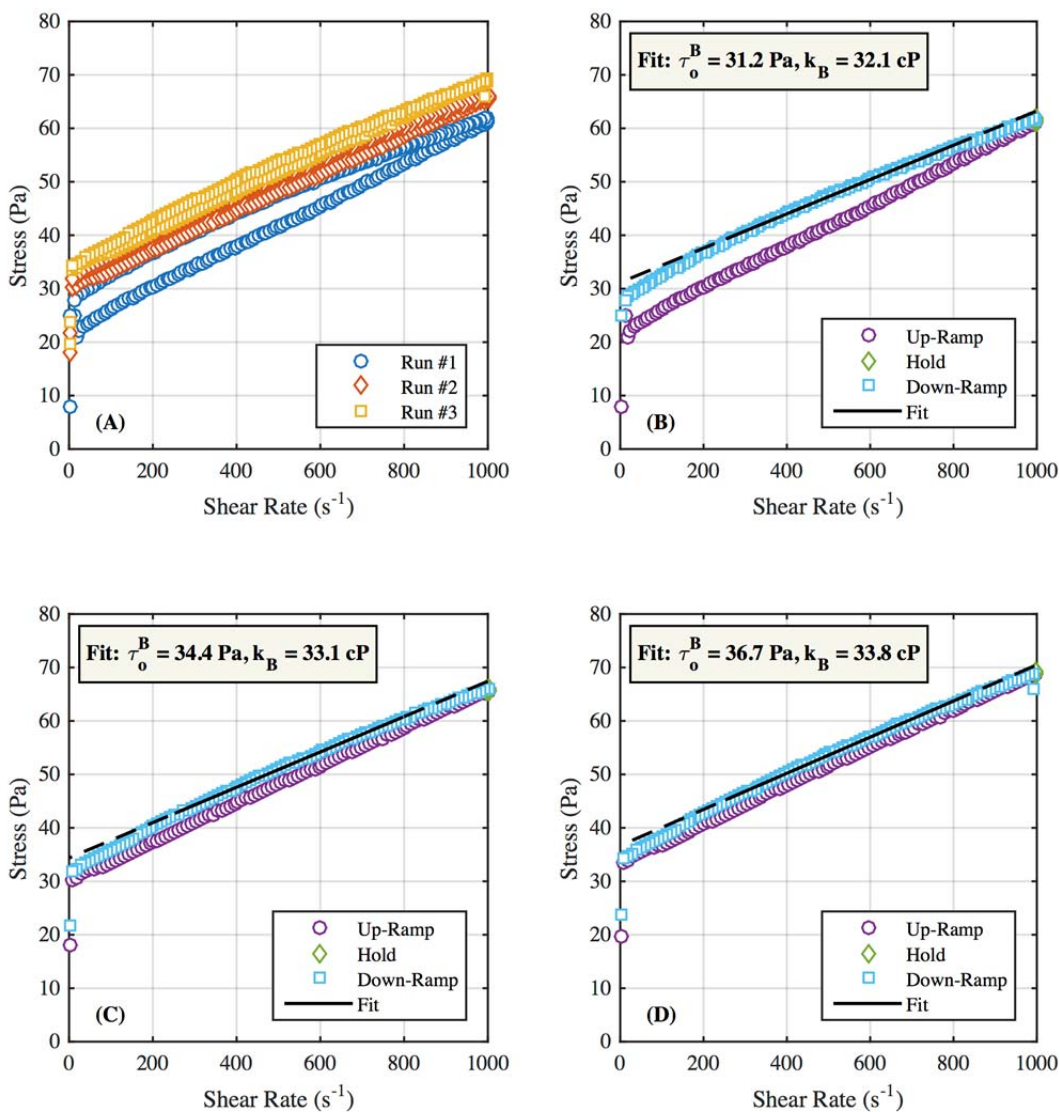


**Figure A.11.** Flow curves for NN-029 after 21 days of aging showing all three consecutive flow curves on the same plot (A) and individually (B – first, C – second, and D – third). Individual flow curves show the best-fit Bingham plastic for a shear rate range of 250 to 800 s<sup>-1</sup> (solid black line) and extrapolated to the full range of shear rates measured (dashed line).

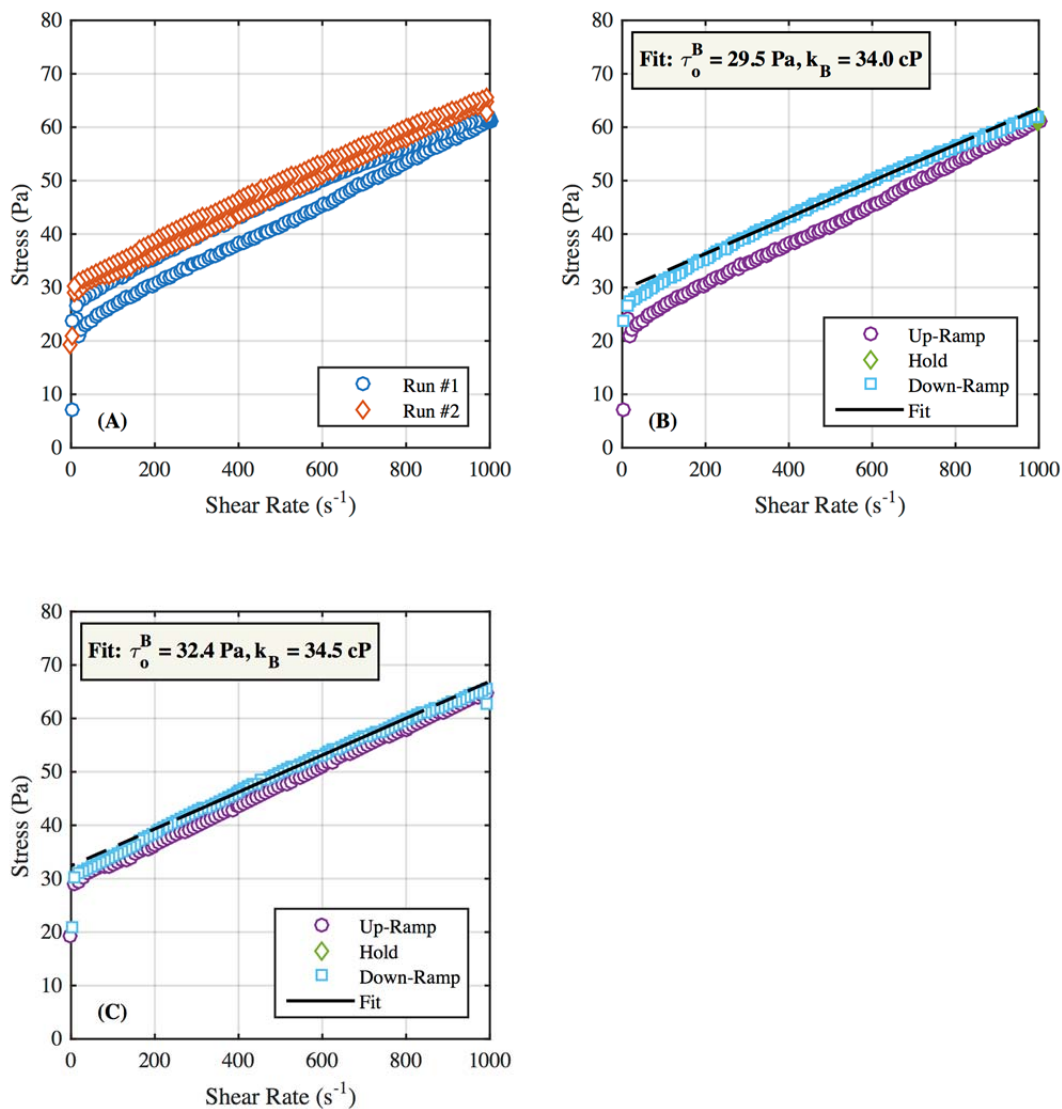


**Figure A.12.** Flow curves for NN-022 after 29 days of aging showing two consecutive flow curves on the same plot (A) and individually (B – first and C – second). Individual flow curves show the best-fit Bingham plastic for a shear rate range of 250 to 800  $s^{-1}$  (solid black line) and extrapolated to the full range of shear rates measured (dashed line).

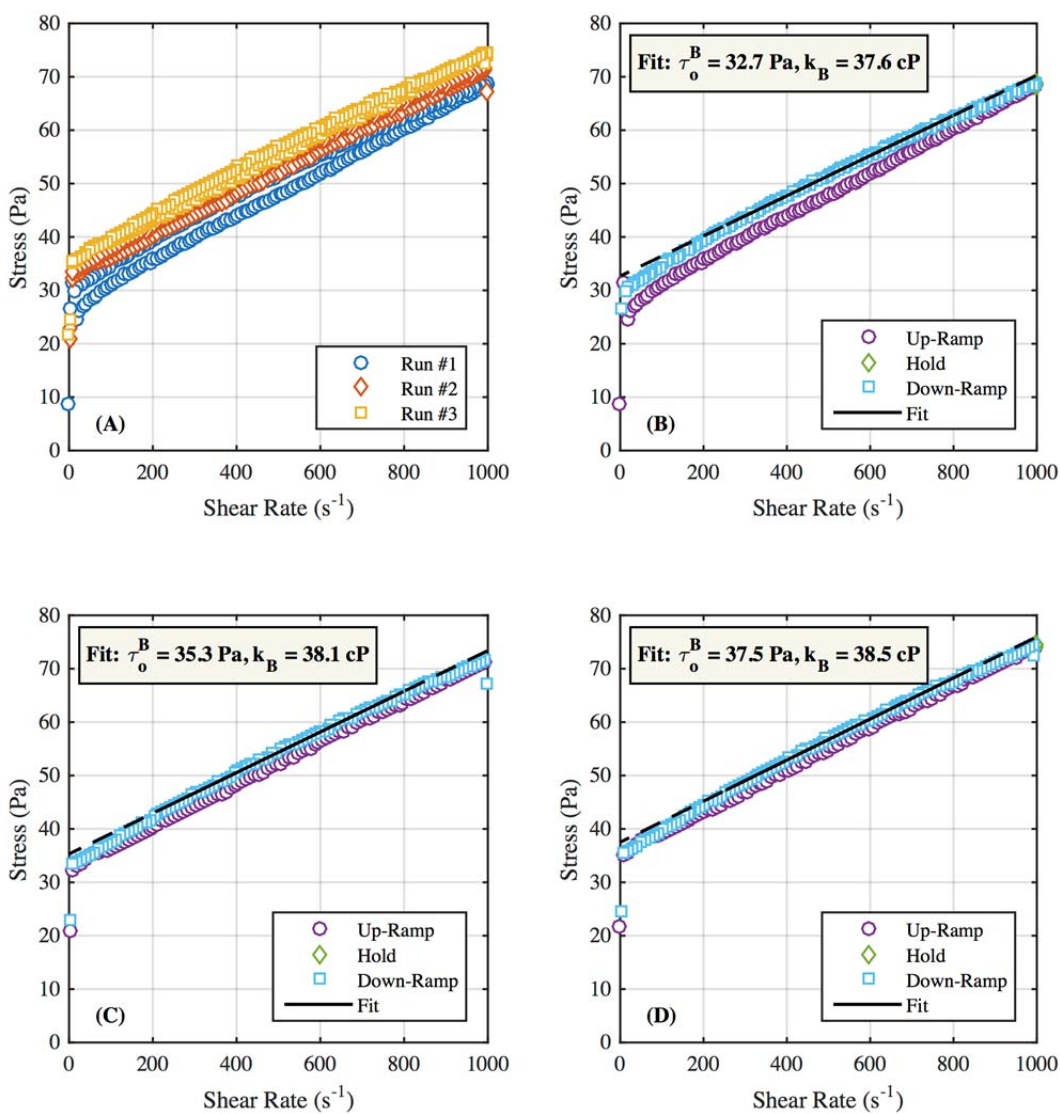


**Figure A.13.** Flow curves for NN-026 after 33 days of aging showing all three consecutive flow curves on the same plot (A) and individually (C – first, C – second, and D – third). Individual flow curves show the best-fit Bingham plastic for a shear rate range of 250 to 800 s<sup>-1</sup> (solid black line) and extrapolated to the full range of shear rates measured (dashed line).

## **Appendix B**

### **Summary of Non-Newtonian Simulant Rheology**



## Appendix B

### Summary of Non-Newtonian Simulant Rheology

Table B.1 provides a summary of rheology for simulants tested during development of the MADC-4 non-Newtonian simulant. All simulants tested are included and indicate the best-fit Bingham plastic constitutive parameters (yield stress and consistency) for the up- and down-shear rate ramps. Fits are limited to shear rates between 250 to 800 s<sup>-1</sup>. It should be noted that this table contains samples that were not discussed in the main body of this report. They are included here to show the full range of simulant and simulant permutations evaluated (for completeness). The rheology data is also limited to the initial rheological measurement made on a particular sample, with a few exceptions. Rheological data measured over time that is reported is limited to those samples that represent the recommended simulant recipe.

**Table B.1.** Summary of initial rheology measurements made during non-Newtonian simulant development.

Sample ID	Description of Nominal Composition	Density (g mL <sup>-1</sup> )	Total Solids (wt%)	Age (d)	Up-Ramp (250 to 800 s <sup>-1</sup> )		Down-Ramp (250 to 800 s <sup>-1</sup> )	
					Yield Stress (Pa)	Consistency (mPa s)	Yield Stress (Pa)	Consistency (mPa s)
NN-001	34 wt% 80:20 clay, 0 wt% NaCl	1.2900	35.49	6.9	15.74	31.65	14.20	32.68
NN-002	35 wt% 80:20 clay, 0 wt% NaCl	1.3021	36.50	6.9	17.12	34.13	16.36	35.30
NN-003	36 wt% 80:20 clay, 0 wt% NaCl	1.3089	37.39	6.8	25.54	42.92	25.55	43.05
NN-004	37 wt% 80:20 clay, 0 wt% NaCl	1.3220	38.61	6.8	31.22	49.71	31.04	51.13
NN-005	34 wt% 80:20 clay, 0.1 wt% NaCl	1.2942	35.86	5.8	22.08	24.42	23.68	23.42
NN-006	35 wt% 80:20 clay, 0.1 wt% NaCl	1.3051	36.78	5.8	26.20	29.12	28.72	27.70
NN-007	36 wt% 80:20 clay, 0.1 wt% NaCl	1.3174	37.90	5.6	37.80	37.76	41.52	35.51
NN-008	37 wt% 80:20 clay, 0.1 wt% NaCl	1.3227	38.70	5.6	49.25	45.04	55.73	41.37
NN-009	34 wt% 80:20 clay, 0.2 wt% NaCl	1.2931	35.87	6.9	28.64	25.07	31.91	23.05
NN-010	35 wt% 80:20 clay, 0.2 wt% NaCl	1.3015	36.64	6.9	29.92	23.81	31.66	23.08
NN-011	36 wt% 80:20 clay, 0.2 wt% NaCl	1.3111	37.51	6.9	43.24	31.62	47.17	29.34
NN-012	37 wt% 80:20 clay, 0.2 wt% NaCl	1.3212	38.53	6.9	58.42	38.72	63.97	35.54
NN-013	34 wt% 80:20 clay, 0.05 wt% NaCl	1.2931	35.76	7.8	16.69	26.36	17.32	25.70
NN-014	35 wt% 80:20 clay, 0.05 wt% NaCl	1.2997	36.49	7.9	21.58	30.35	23.74	28.78
NN-015	36 wt% 80:20 clay, 0.05 wt% NaCl	1.3093	37.69	7.9	28.73	35.81	30.14	34.63
NN-016	37 wt% 80:20 clay, 0.05 wt% NaCl	1.3215	38.57	8.0	40.98	46.09	43.52	44.19
NN-017	35.7 wt% 80:20 clay, 0.08 wt% NaCl	1.3101	37.49	7.8	28.76	34.16	32.11	32.47
NN-018	35.7 wt% 80:20 clay, 0.08 wt% NaCl	1.3065	37.26	7.8	28.02	32.82	31.21	31.15
NN-019	35.7 wt% 80:20 clay, 0.08 wt% NaCl	1.3050	37.43	8.0	30.51	35.92	33.60	34.27
NN-020	35.5 wt% 80:20 clay, 0.08 wt% NaCl	1.3046	37.42	7.9	28.97	34.47	32.06	32.66
NN-021	35.9 wt% 80:20 clay, 0.08 wt% NaCl	1.3089	37.54	7.9	33.76	36.82	36.82	35.10
NN-022	35.7 wt% 80:20 clay, 0.09 wt% NaCl	1.3067	37.60	7.9	31.23	34.32	35.71	31.85
NN-023	35.7 wt% 80:20 clay, 0.07 wt% NaCl	1.3055	37.22	8.0	28.41	31.84	30.19	31.30
NN-024	35.8 wt% 80:20 clay, 0.085 wt% NaCl	1.3090	37.11	2.8	41.09	36.34	43.84	34.39
NN-025	35.5 wt% 80:20 clay, 0.085 wt% NaCl	1.3056	36.84	2.9	39.04	34.33	41.04	33.09

Sample ID	Description of Nominal Composition	Density (g mL <sup>-1</sup> )	Total Solids (wt%)	Age (d)	Up-Ramp (250 to 800 s <sup>-1</sup> )		Down-Ramp (250 to 800 s <sup>-1</sup> )	
					Yield Stress (Pa)	Consistency (mPa s)	Yield Stress (Pa)	Consistency (mPa s)
NN-026	35.7 wt% 80:20 clay, 0.09 wt% NaCl	1.3139	37.24	2.9	40.81	35.20	43.35	33.54
NN-027	35.7 wt% 80:20 clay, 0.09 wt% NaCl	1.3128	38.07	7.8	31.34	35.35	35.36	33.38
NN-028	35.7 wt% 80:20 clay, 0.09 wt% NaCl [LDSP added after clay aging]	1.3094	37.76	9.8	33.56	32.03	35.18	31.25
NN-029	35.7 wt% 80:20 clay, 0.09 wt% NaCl [no LDSP added]	1.2747	35.52	7.9	29.62	33.94	33.28	30.45
NN-030	35.7 wt% 80:20 clay, 0.09 wt% NaCl [NaCl added after clay aging]	1.3077	37.56	9.9	29.85	43.02	29.40	44.01
NN-031	35.7 wt% 80:20 clay, 0.09 wt% NaCl [both NaCl and LDSP added after clay aging]	1.3076	37.51	11.9	59.19	50.20	63.96	47.51
NN-032	35.7 wt% 80:20 clay, 0.09 wt% NaCl [no LDSP and NaCl added after clay aging]	1.2733	35.19	9.9	30.08	42.12	29.76	42.72
NN-033	35.7 wt% 80:20 clay, 0.09 wt% NaCl	1.3046	37.12	22.3	34.47	33.8	39.18	30.9
NN-033-0.3	36.0 wt% 80:20 clay, 0.09 wt% NaCl [water withheld]	1.3030	37.62	22.4	37.62	37.85	43.97	32.28
NN-033-100	35.7 wt% 80:20 clay, 0.09 wt% NaCl	1.3067	37.11	2.8	32.21	32.81	37.35	29.02
NN-034	35.7 wt% 80:20 clay, 0.09 wt% NaCl	1.3066	37.13	26.1	35.47	34.54	40.00	32.01
NN-034-0.5	36.2 wt% 80:20 clay, 0.09 wt% NaCl [water withheld]	1.3123	37.72	25.4	35.11	37.15	40.91	33.48
NN-034-100	35.7 wt% 80:20 clay, 0.09 wt% NaCl	1.3049	37.14	2.8	32.89	33.93	38.01	30.94
NN-027	35.7 wt% 80:20 clay, 0.09 wt% NaCl	1.3128		49.9	32	37.65	33.75	36.49
NN-027-D10	NN-027 diluted to a dilution ratio of ~10%	1.2943	35.80	NA	12.11	20.49	12.77	21.51
NN-027-D20	NN-027 diluted to a dilution ratio of ~20%	1.2645	33.00	NA	5.058	11.31	5.155	11.73
NN-029	35.7 wt% 80:20 clay, 0.09 wt% NaCl [no LDSP added]	1.2747	-- --	50.9	32.73	38.95	36.8	36.75

Sample ID	Description of Nominal Composition	Density (g mL <sup>-1</sup> )	Total Solids (wt%)	Age (d)	Up-Ramp (250 to 800 s <sup>-1</sup> )		Down-Ramp (250 to 800 s <sup>-1</sup> )	
					Yield Stress (Pa)	Consistency (mPa s)	Yield Stress (Pa)	Consistency (mPa s)
NN-029C	35.7 wt% 80:20 clay, 0.09 wt% NaCl [no LDSP added]	1.2692	34.84	26.1	37.26	39.45	41.53	36.78
NN-027-10C	35.7 wt% 80:20 clay, 0.09 wt% NaCl, measured at 10°C	---	---	67.0	38.88	60.14	42.11	58.7
NN-027-15C	35.7 wt% 80:20 clay, 0.09 wt% NaCl, measured at 15°C	---	---	67.0	35.41	53.73	39.18	51.22
NN-027-20C	35.7 wt% 80:20 clay, 0.09 wt% NaCl, measured at 20°C	---	---	67.1	35.85	49.51	39.24	47.92
NN-027-25C	35.7 wt% 80:20 clay, 0.09 wt% NaCl, measured at 25°C	---	---	67.1	35.76	44.44	39.25	43.41
NN-027-30C	35.7 wt% 80:20 clay, 0.09 wt% NaCl, measured at 30°C	---	---	67.1	37.54	41.69	42.05	39.83
NN-029-10C	35.7 wt% 80:20 clay, 0.09 wt% NaCl [no LDSP], measured at 10°C	---	---	70.2	38.68	58.43	42.15	56.64
NN-029-15C	35.7 wt% 80:20 clay, 0.09 wt% NaCl [no LDSP], measured at 15°C	---	---	70.1	33.58	48.76	37.54	46.39
NN-029-20C	35.7 wt% 80:20 clay, 0.09 wt% NaCl [no LDSP], measured at 20°C	---	---	70.0	32.01	42.48	35.38	41.05
NN-029-25C	35.7 wt% 80:20 clay, 0.09 wt% NaCl [no LDSP], measured at 25°C	---	---	70.0	31.46	37.72	34.9	35.91
NN-029-30C	35.7 wt% 80:20 clay, 0.09 wt% NaCl [no LDSP], measured at 30°C	---	---	69.9	33.31	37.25	38.31	34.54
NN-027C	35.7 wt% 80:20 clay, 0.09 wt% NaCl	---	---	7.8	35.07	32.87	37.15	31.85
NN-027C	35.7 wt% 80:20 clay, 0.09 wt% NaCl	1.3073	37.21	16.0	17.62	31.05	29.65	30.04
NN-027C-D20	NN-027C diluted to a dilution ratio of 10%	1.2530	31.70	0.2	5.196	10.59	5.106	10.92
NN-027C-D10	NN-027C diluted to a dilution ratio of 20%	1.2817	34.87	0.1	10.37	15.09	10.21	15.62

Sample ID	Description of Nominal Composition	Density (g mL <sup>-1</sup> )	Total Solids (wt%)	Age (d)	Up-Ramp (250 to 800 s <sup>-1</sup> )		Down-Ramp (250 to 800 s <sup>-1</sup> )	
					Yield Stress (Pa)	Consistency (mPa s)	Yield Stress (Pa)	Consistency (mPa s)
NN-028	35.7 wt% 80:20 clay, 0.09 wt% NaCl [LDSP added after clay aging], measured at 25°C	---	---	80.1	31.6	38.81	34.93	37.72
NN-028-10C	35.7 wt% 80:20 clay, 0.09 wt% NaCl [LDSP added after clay aging], measured at 10°C	---	---	80.9	37.26	57.95	40.78	55.82
NN-028-15C	35.7 wt% 80:20 clay, 0.09 wt% NaCl [LDSP added after clay aging], measured at 15°C	---	---	80.8	34.24	50.65	37.69	48.93
NN-028-20C	35.7 wt% 80:20 clay, 0.09 wt% NaCl [LDSP added after clay aging], measured at 20°C	---	---	79.1	33.15	45.27	36.67	43.91
NN-028-30C	35.7 wt% 80:20 clay, 0.09 wt% NaCl [LDSP added after clay aging], measured at 30°C	---	---	80.9	31.93	36.28	34.86	35.53
NN-027-DI	35.7 wt% 80:20 clay, 0.09 wt% NaCl [prepared with DI water instead of RCW]	1.3053	37.21	15.0	37.4	36.49	39.88	35.53



## Distribution

**No. of  
Copies**

**No. of  
Copies**

**8 Bechtel National Inc.**

Steve Barnes	PDF
William Donigan	PDF
Jeff Monahan	PDF
Bob Voke	PDF
Fred Damerow	PDF
Paul Townson	PDF
Dan Herting	PDF

**10 Pacific Northwest National Laboratory**

CA Burns	PDF
RC Daniel	PDF
PA Gauglitz	PDF
SD Hoyle	PDF
RA Peterson	PDF
KP Recknagle	PDF
PP Schonewill	PDF
BE Wells	PDF
Information Release	PDF
Project File	PDF







**Pacific Northwest**  
NATIONAL LABORATORY

*Proudly Operated by **Battelle** Since 1965*

902 Battelle Boulevard  
P.O. Box 999  
Richland, WA 99352  
1-888-375-PNNL (7665)

U.S. DEPARTMENT OF  
**ENERGY**

---

[www.pnnl.gov](http://www.pnnl.gov)